THE UTILIZATION OF THE EXHAUST GAS ENERGY OF A TWO-STROKE DIESEL ENGINE

John D. Crowley
Arthur W. Gottschalk
William R. Nodell

54

THE UTILIZATION OF THE EXHAUST GAS ENERGY OF A TWO-STROKE DIESEL ENGINE

by

Lieutenant John D. Crowley, United States Coast Guard

Lieutenant Arthur W. Gottschalk, United States Navy

Lieutenant William R. Nodell, United States Coast Guard

Submitted to the
Department of Naval Architecture and Marine Engineering
on
20 May 1957
in partial fulfillment of the requirements for the
Degree of Naval Engineer
at the
Massachusetts Institute of Technology

T-ficaa
C92

THE UTILIZATION OF THE EXHAUST GAS ENERGY OF A TWO-STROKE DIESEL ENGINE

by

Lieutenant John D. Crowley, United States Coast Guard

Lieutenant Arthur W. Gottschalk, United States Navy

Lieutenant William R. Nodell, United States Coast Guard

Submitted to the
Department of Naval Architecture and Marine Engineering
on
20 May 1957
in partial fulfillment of the requirements for the
Degree of Naval Engineer
at the
Massachusetts Institute of Technology

Cambridge, Massachusetts

May 20, 1957

Secretary of the Faculty
Massachusetts Institute of Technology
Cambridge 39, Massachusetts

Dear Sir:

The attached thesis entitled "Utilization of Exhaust Gas Energy of a Two-Stroke Diesel Engine" is herewith submitted in partial fulfillment of the requirements of the Degree of Naval Engineer.

Respectfully,

Lt. John D. Crowley, USCG

Lt. Arthur W. Gottschalk, USN

Lt. William R. Nodell, USCG

ABSTRACT

UTILIZATION OF THE EXHAUST GAS ENERGY OF A TWO-STROKE DIESEL ENGINE

Submitted to the Department of Naval Architecture and Marine Engineering on 20 May 1957 in partial fulfillment of the requirements for the Degree of Naval Engineer.

An experimental study was made of the effect of turbocharger nozzle area upon the total output and the brake specific fuel consumption of a two-stroke diesel engine, GM 3-71. Compressor power requirements were predicted from air flow measurements while turbine output predictions were based on measurements of exhaust gas momentum after leaving the exhaust nozzles. Engine power outputs were measured directly.

It was found that total power increases monotonically as nozzle area decreases, but that an optimum brake specific fuel consumption is obtained with a nozzle such that nozzle area/piston area is 0.10.

Recommendations are made that further study be made to determine if the optimum shifts as piston speed or compression ratio changes. It is also recommended that a study of exhaust valve area be made, as an increase of exhaust area seems indicated to improve supercharged performance.

Thesis Supervisor: C. F. Taylor, Professor, Mechanical Engineering

ACKNOWLEDGEMENTS

The authors would like to express their appreciation for the aid and advice given them by the Faculty and Staff of the Sloan Automotive Laboratory of the Institute.

Particular credit and thanks are given to Professor C. F. Taylor, Associate Professors K. R. Wadleigh and A. R. Rogowski, and Mr. James C. Livengood for their help, suggestions, and criticism without which this work would not have been possible.

In addition we would like to thank Professors W. M. Murray and F. M. Lewis for their valuable advice on special problems which arose.

TABLE OF CONTENTS

LIST OF FIGURES ii

LIST OF SYMBOLS iv

I. INTRODUCTION 1

II. PROCEDURE 3

III. RESULTS 6

IV. DISCUSSION OF RESULTS 7

V. CONCLUSIONS 10

VI. RECOMMENDATIONS 11

VII. APPENDICES

A. THE USE OF A FLAT PLATE TO MEASURE THE WORK A TURBINE COULD REMOVE FROM A CYCLIC JET FLOW 18

B. DETAILS OF PROCEDURE 34

C. SUMMARY OF DATA 40

D. SUMMARY OF CALCULATIONS 55

E. ENGINE FRICTION 65

G. SUPPLEMENTARY DISCUSSION 68

H. BIBLIOGRAPHY 72

LIST OF FIGURES

Figure I, Reversible Mean Effective Pressures as Functions of Nozzle Areas 7

Figure II, Brake Mean Effective Pressures as Functions of Nozzle Areas 8

Figure III, Brake Specific Fuel Consumption as Function of Nozzle Area 9

Figure IV, Brake Specific Fuel Consumption as Function of Nozzle Area 10

Figure V, Comparison of Turbine and Compressor Work for Nozzles 0.20 and 0.10 11

Figure VI, Comparison of Turbine and Compressor Work for Nozzles 0.05 and 0.025 12

Figure VII, Control Volume for Flat Plate Analysis 18

Figure VIII, Turbine Velocity Diagram 20

Figure IX, Force Plate Instrumentation 24

Figure X, Strain Gage Circuit 25

Figure XI, Instantaneous Pressure and Jet Force 32

Figure XII, Equipment Schematic 35

Figure XIII, Exhaust Pipe Arrangement 37

Figure XIV, Nozzle Dimensions 38

Figure XV, Sample Exhaust Pipe Pressure Cards 45

Figure XVI, Cross Curves of $(IMEP)_R$ vs. F/A, for Nozzle 0.20 51

Figure XVII, Cross Curves of $(IMEP)_R$ vs. F/A, for Nozzle 0.10 52

Figure XVIII, Cross Curves of $(IMEP)_R$ vs. F/A, for Nozzle 0.05 53

Figure XIX, Cross Curves of $(IMEP)_R$ vs. F/A, for Nozzle 0.025 54

Figure XX, Uncorrected Air Flow Through the Metering Orifice 56

Figure XXI, Expansion Factor Y for Correcting Air Flow 57

Figure XXII, Scavenge Efficiency of the GM 3-71 Engine 58

Figure XXIII, Calculation Curve for Turbine Horsepower 60

Figure XXIV, Calculation Curve for Compressor Horsepower 61

Figure XXV, Calculation Curve for Jet Force from Stagnation Pressure 64

Figure XXVI, Friction Horsepower 66

Figure XXVII, Friction Horsepower 67

LIST OF SYMBOLS

BHP_T	Total brake horsepower from $BMEP_T$ (h.p.)
$BMEP_M$	Measured brake mean effective pressure from the dynamometer (psi)
$BMEP_T$	Total brake mean effective pressure = $IMEP_E$ - 1/3 FMEP + TMEP - CMEP (psi)
BSFC	Brake specific fuel consumption $\frac{(\text{lbs fuel})}{(BHP_T - \text{hr})}$
CHP_R	Compressor horsepower isentropic (h.p.)
CMEP	Compressor mean effective pressure @η_c = 0.75 (psi)
$CMEP_R$	Compressor mean effective pressure isentropic (psi)
F	Mean time averaged force of exhaust gas (lb)
F/A	Cylinder fuel-air ratio (dimensionless)
FMEP	Measured friction mean effective pressure for three cylinders (psi)
$IMEP_E$	Engine indicated mean effective pressure = $BMEP_M$ + FMEP (psi)
$IMEP_R$	Total indicated mean effective pressure isentropic = $IMEP_E$ + $TMEP_R$ - $CMEP_R$ (psi)
K	Ratio of specific heats (dimensionless)
M_A	Mass flow rate of air (lb/sec)
M_F	Mass flow rate of fuel (lb/sec)
N	Engine revolutions per minute
P_A	Stagnation pressure before the nozzle (psia or "H_G abs)
P_{ATM}	Barometric pressure ("H_G gage)
P_B	Static pressure downstream of nozzle (psia or "H_G abs)
P_{E_1}	Static pressure in exhaust pipe ("H_G gage)

P_{E2}	Pressure in exhaust receiver ("H_G gage)
Pi	Pressure in inlet receiver ("H_G gage)
P_{OIL}	Oil pressure in engine (psi)
P_R	Pressure ratio for compressor work $\frac{(pi + P_{ATM})}{(P_{ATM})}$ (dimensionless)
P_1	Pressure before the air flow measuring orifice ("H_G gage)
ΔP	Pressure across the flow measuring orifice ("H_2O)
R	Gas constant for air 53.3 $\frac{ft - lb\ force}{°R - lb\ mass}$
R	Electrical resistance (ohms)
R_S	Scavenging ratio $60\ M_A/\rho_S\ N\ Vc$ (dimensionless)
T_E	Exhaust temperature in pipe (°F)
T_J	Engine water jacket temperature (°F)
T_1	Inlet air temperature before orifice (°F)
THP_R	Turbine horsepower isentropic (h.p.)
TMEP	Turbine mean effective pressure @η_T = 0.75 (psi)
$TMEP_R$	Turbine mean effective pressure isentropic (psi)
V_C	Total cylinder volume at bottom center (ft^3)
ϵ	Strain (in/in)
Γ	Trapping efficiency η_S/R_S (dimensionless)
η_C	Compressor efficiency (dimensionless)
η_S	Scavenging efficiency = fresh air trapped in cylinder ÷ $\rho_S\ V_C$ (dimensionless)
η_T	Turbine efficiency (dimensionless)
ρ_S	Scavenging density = $\frac{(0.491)(P_{E1} + P_{ATM})(144)}{R\ (T_1 + 460)}$ $\frac{(lb)}{(\overline{ft^3})}$
σ	Stress (psi)

INTRODUCTION

The output of an internal combustion engine is limited by its air capacity. In order to increase the air capacity and hence the output, engines are supercharged. While both supercharged four-stroke and two-stroke diesel engines have been widely employed, the nature of the air flow process in the two-stroke engine makes the supercharged engine design a very difficult problem. The four-stroke engine air capacity is insensitive to changes in exhaust pressure, but the air capacity of the two-stroke engine is equally sensitive to changes in inlet and exhaust pressures. Analytical studies have been and are being made of two-stroke flow processes, but both their complexity and uncertainty have thus far precluded their use by the designer. As a result, the design of the air flow features of two-stroke engines is done by empirical and experimental methods.

If we consider supercharging an existing two-stroke engine merely by raising the inlet pressure, we will find little, if any, gain in net engine output. The air flow through the engine will increase largely, requiring a large compressor power for supercharging. However, it will be found that most of this air blows through the engine with only a small increase in the charge trapped in the cylinder. In order to effectively supercharge, it is necessary to raise the exhaust as well as the inlet pressure. This immediately suggests the use of an exhaust gas turbine with the engine; the turbine producing the increase of exhaust pressure needed and recovering some of the exhaust gas energy for use in compressing the inlet air.

An important variable in the design of such a turbocharger arrangement is the area of the turbine nozzle. Inasmuch as it affects not only the flow process in the turbine, but also has a marked effect upon the air flow of the engine, the nozzle choice will affect compressor work requirements, engine air capacity, and turbine output. This thesis is an experimental study of the effects of changes of exhaust gas turbine nozzle area upon the net output of a supercharged, two-stroke diesel engine.

PROCEDURE

The experimental study was conducted on one cylinder of a General Motors 3-71 diesel engine, fitted with an exhaust pipe to which nozzles of various areas could be attached. Tests were run with four different nozzles, with areas chosen so that the ratio of nozzle throat area to piston area was: 0.20; 0.10; 0.05; 0.025. The two cylinders of the engine which were not fitted with the special exhaust and nozzle were blanked off at the exhaust, and operated with the pistons in place, but with the cylinders not firing and no air flow through the cylinders. For the details of the engine, exhaust pipe, nozzles and instrumentation, see Appendix B.

The engine was run over a wide range of fuel-air ratios and scavenge ratios with each nozzle, at a piston speed of 1335 fpm (1600 rpm). The ranges covered were approximately as shown in Table I.

TABLE I

Range of Experiments

Nozzle (Area Ratio)	Fuel-Air Ratio Range	Scavenge Ratio Range
0.20	0.025 - 0.040	1.0 - 1.5
0.10	0.025 - 0.040	1.0 - 1.5
0.05	0.025 - 0.040	1.0 - 1.5
0.025	0.025 - 0.040	1.0

The smallest nozzle was not run at higher scavenge ratios than 1.0, as at that scavenge ratio and at fuel air ratios of 0.035 to 0.040 the engine was laboring heavily and operating at a mean effective pressure far in excess of its rated value. At higher scavenge ratios, the overloading would have been excessive.

Prior to the test runs, the friction power of the engine was determined by motoring the engine at various speeds and inlet pressures. In addition, motoring friction was determined for a number of runs by comparing indicated pressure from pressure-crank angle diagrams with the brake mean effective pressure measured with the engine dynamometer.

At each operating point, the air and fuel flows, inlet and exhaust pressures, and brake power output were measured. In addition, engine cylinder pressures, and stagnation and static pressures in the exhaust pipe were recorded as crank angle--pressure diagrams. A force plate deflected the exhaust gas discharging from the nozzle, and the force exerted by this impinging gas jet was recorded. From the brake power and the earlier friction power, the engine indicated mean effective pressure was computed. The necessary compressor power was computed from the air flow and the inlet air pressure to atmospheric pressure ratio. Appendix A indicates the method used to compute the turbine work from the jet force and the air and fuel flows.

From the above data, the net indicated mean effective pressure of the combined unit was computed. In order to facilitate plotting, those series of runs which were taken at essentially constant scavenge ratio were plotted as lines of constant scavenge ratio on an IMEP vs. fuel-air ratio axis. One series of runs was taken, essentially at constant engine BMEP. These runs were originally plotted as lines of constant engine BMEP on an IMEP vs. scavenge ratio axis and on fuel-air ratio vs. scavenge ratio axis. In each case, engine, compressor, and turbine IMEP were separately plotted. The results of these cross plots were then plotted as lines of constant scavenge ratio on the IMEP vs. fuel-air ratio graph. The final plots were prepared by plotting, from the

IMEP vs. fuel-air ratio graphs for each nozzle, the total IMEP value as a function of nozzle area for fixed values of scavenge ratio and fuel-air ratio. In a similar manner, brake mean effective pressure plots were prepared. These were done on the following basis:

a. One-third the total engine friction mean effective pressure was deducted from the cylinder mean effective pressure to give brake mean effective pressure.

b. The compressor efficiency was assumed to be 0.75.

c. The turbine efficiency was assumed to be 0.75.

Brake specific fuel consumption was predicted from the faired values of the BMEP plots on the basis of the fuel-air ratios plotted and measured air flows and scavenge ratios.

RESULTS

The results of this study are presented in six graphs, Figures I through VI.

Figure I presents IMEP (engine IMEP plus turbine IMEP minus compressor IMEP) plotted as a function of nozzle area for constant values of scavenge ratio and fuel-air ratio.

Figure II presents BMEP (engine BMEP plus turbine BMEP minus compressor BMEP) plotted as a function of nozzle area for constant values of scavenge ratio and fuel-air ratio.

Figures III and IV present BSFC as a function of nozzle area for constant values of scavenge ratio and fuel-air ratio.

Figures V and VI present a plot of the ratio of turbine BMEP less compressor BMEP to the total BMEP as functions of fuel-air ratio, for each nozzle at specific scavenge ratios.

FIGURE I

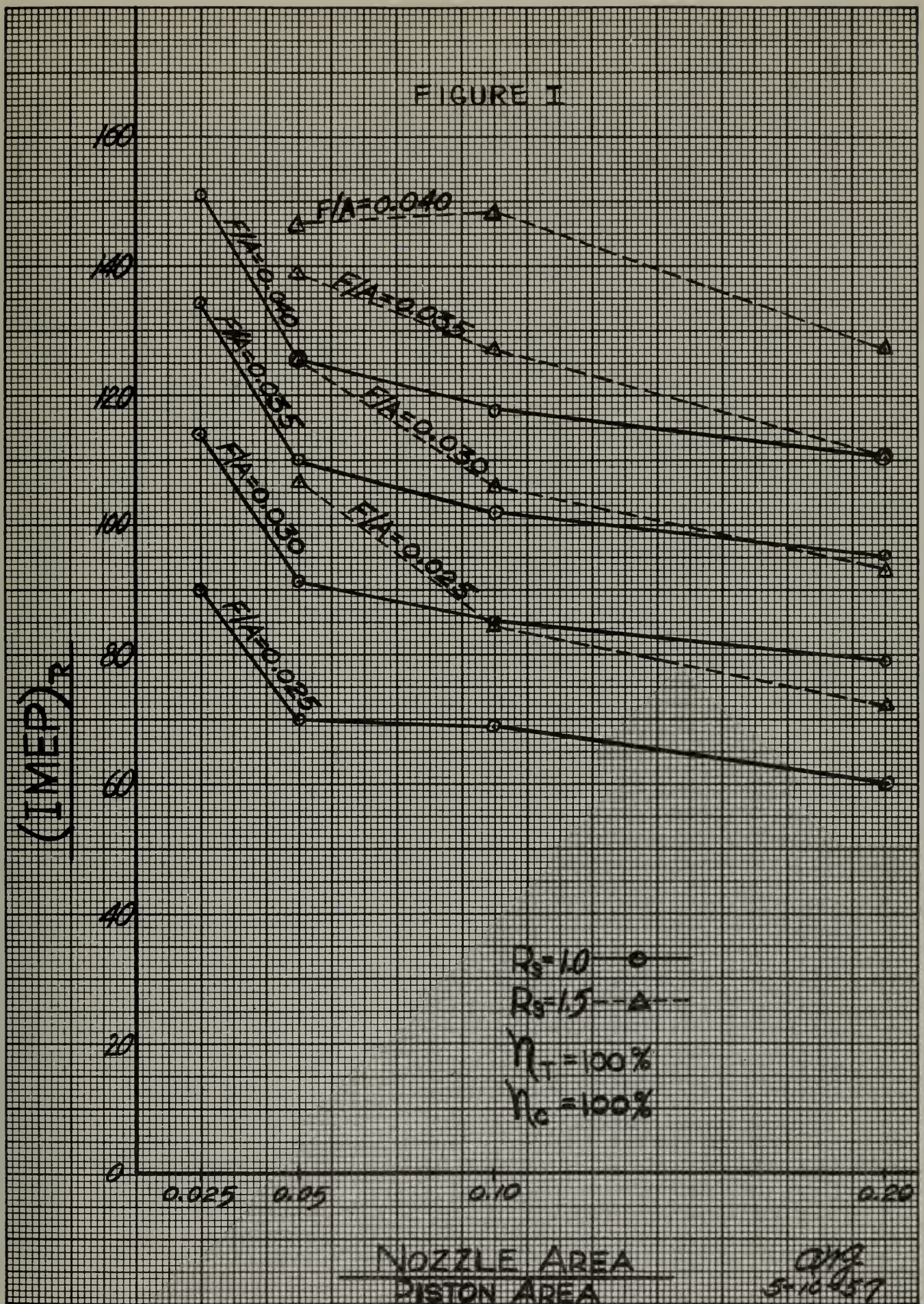
160
140
120
100
80
60
40
20
0
(IMEP)R
F/A=0.040
F/A=0.035
F/A=0.030
F/A=0.025
F/A=0.040
F/A=0.035
F/A=0.030
F/A=0.025
Rs=1.0
Rs=1.5
ηT=100%
ηc=100%
0.025
0.05
0.10
0.20
NOZZLE AREA
PISTON AREA
5-10-57

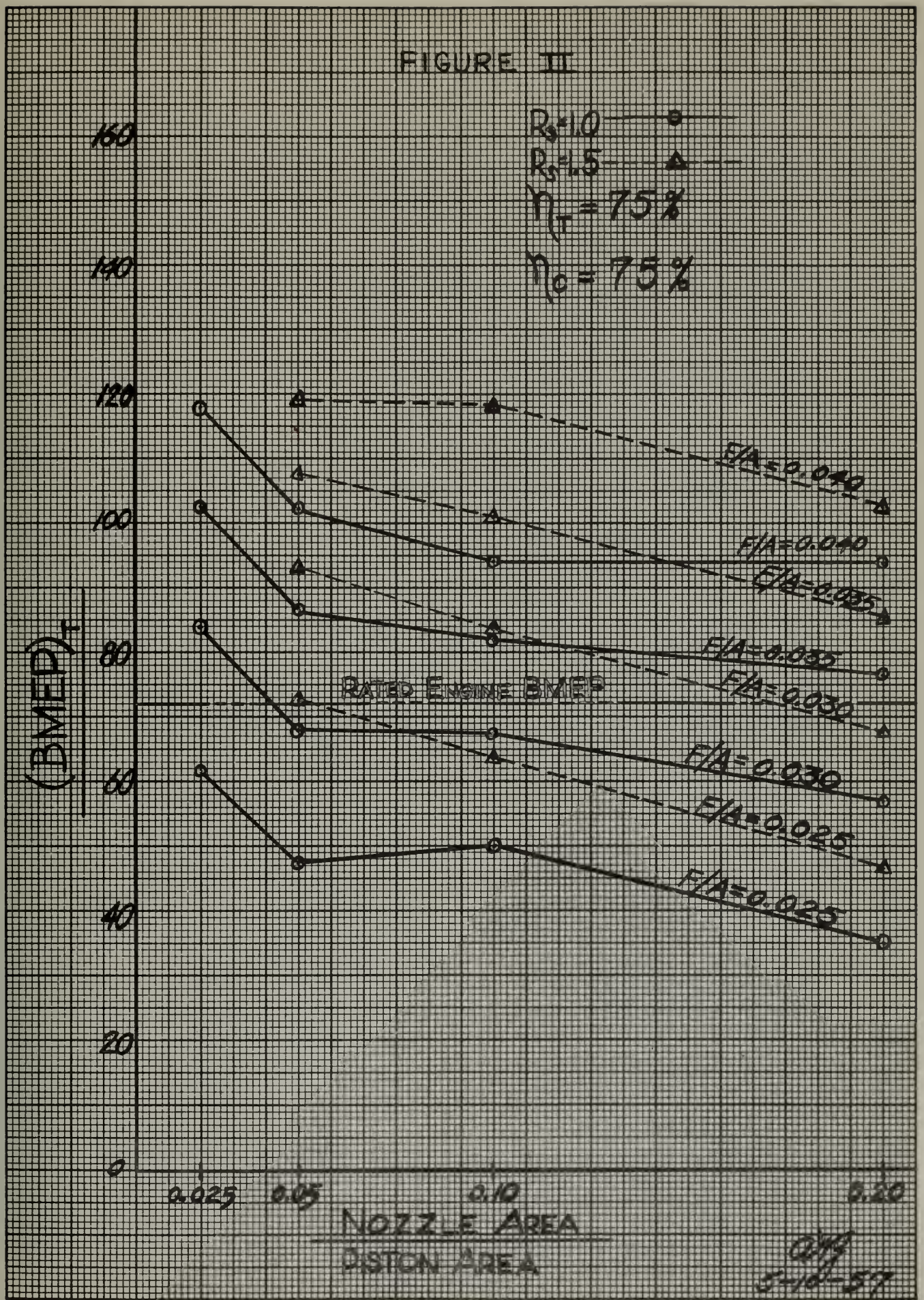
FIGURE II
R_s=1.0
R_s=1.5
η_T = 75%
η_C = 75%
F/A=0.040
F/A=0.040
F/A=0.035
F/A=0.030
F/A=0.030
F/A=0.025
F/A=0.020
RATED ENGINE BMEP
(BMEP)$_T$
160
140
120
100
80
60
40
20
0
0.025
0.05
0.10
0.20
NOZZLE AREA
PISTON AREA
5-10-57

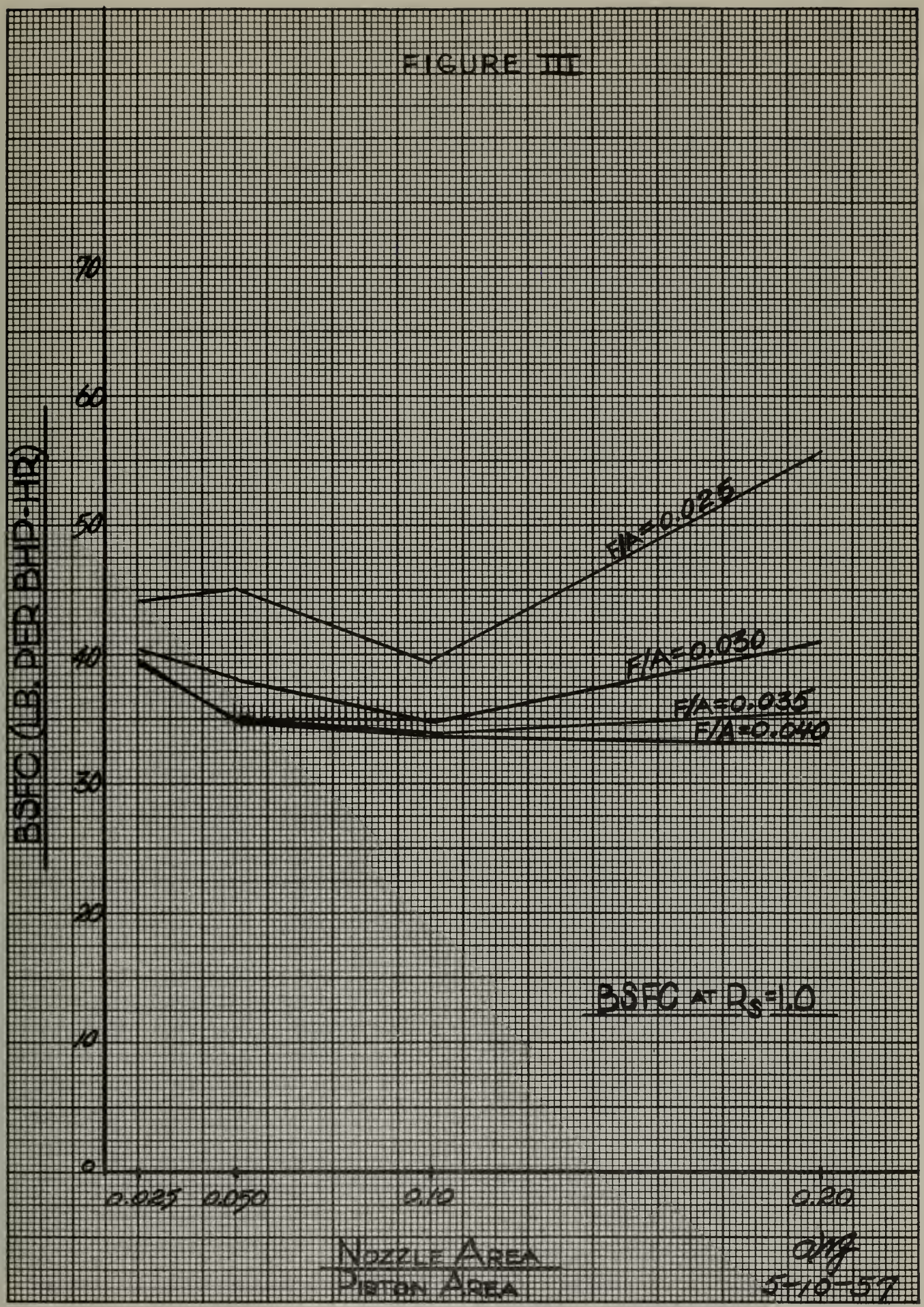
FIGURE III
BSFC (LB. PER BHP-HR)
70
60
50
40
30
20
10
0
F/A=0.025
F/A=0.030
F/A=0.035
F/A=0.040
BSFC AT R_S=1.0
0.025
0.050
0.10
0.20
NOZZLE AREA
PISTON AREA
5-10-57

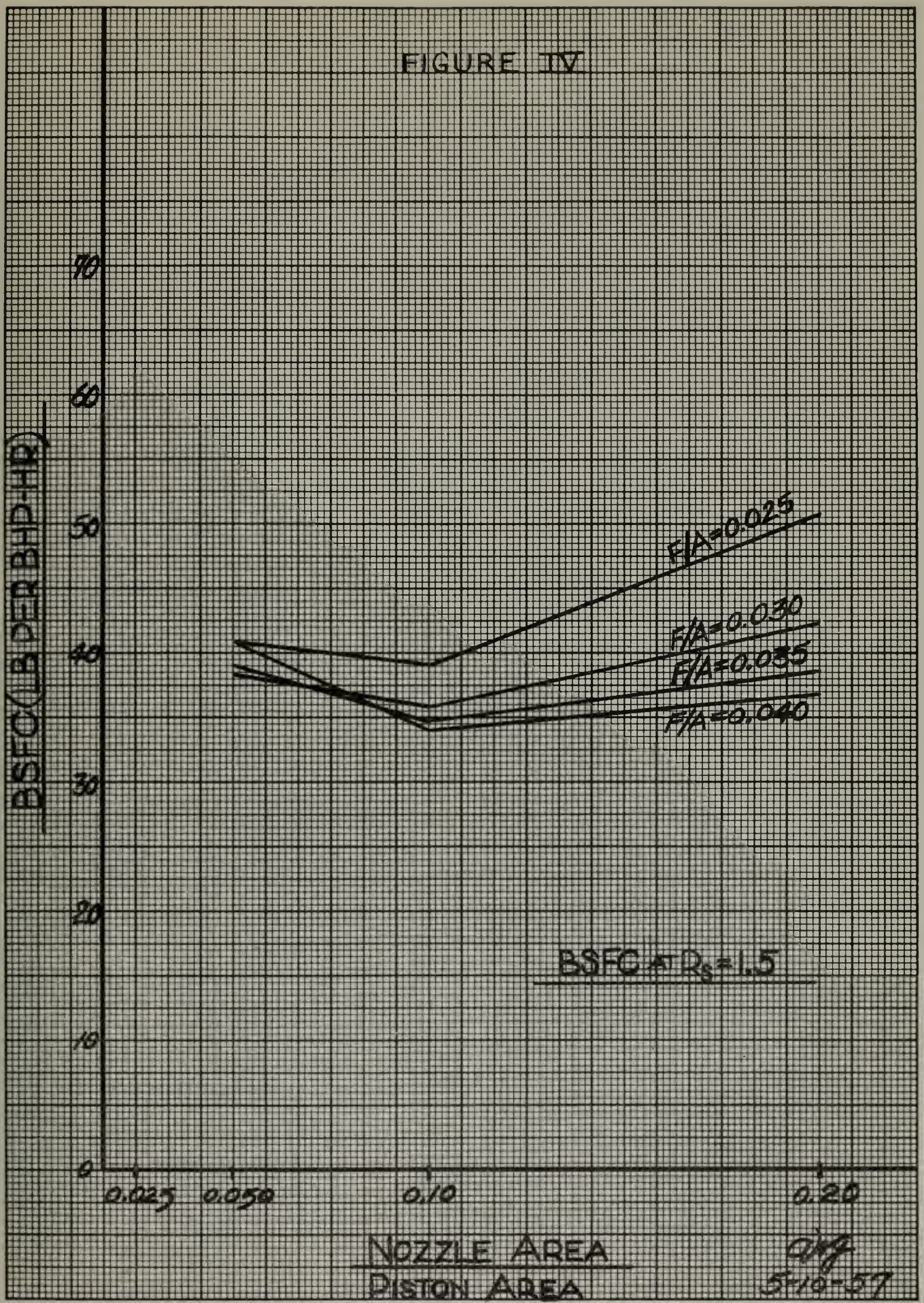
FIGURE IV
BSFC (LB PER BHP-HR)
70
60
50
40
30
20
10
0
F/A=0.025
F/A=0.030
F/A=0.035
F/A=0.040
BSFC AT Rs = 1.5
0.025
0.050
0.10
0.20
NOZZLE AREA
PISTON AREA
5-19-57

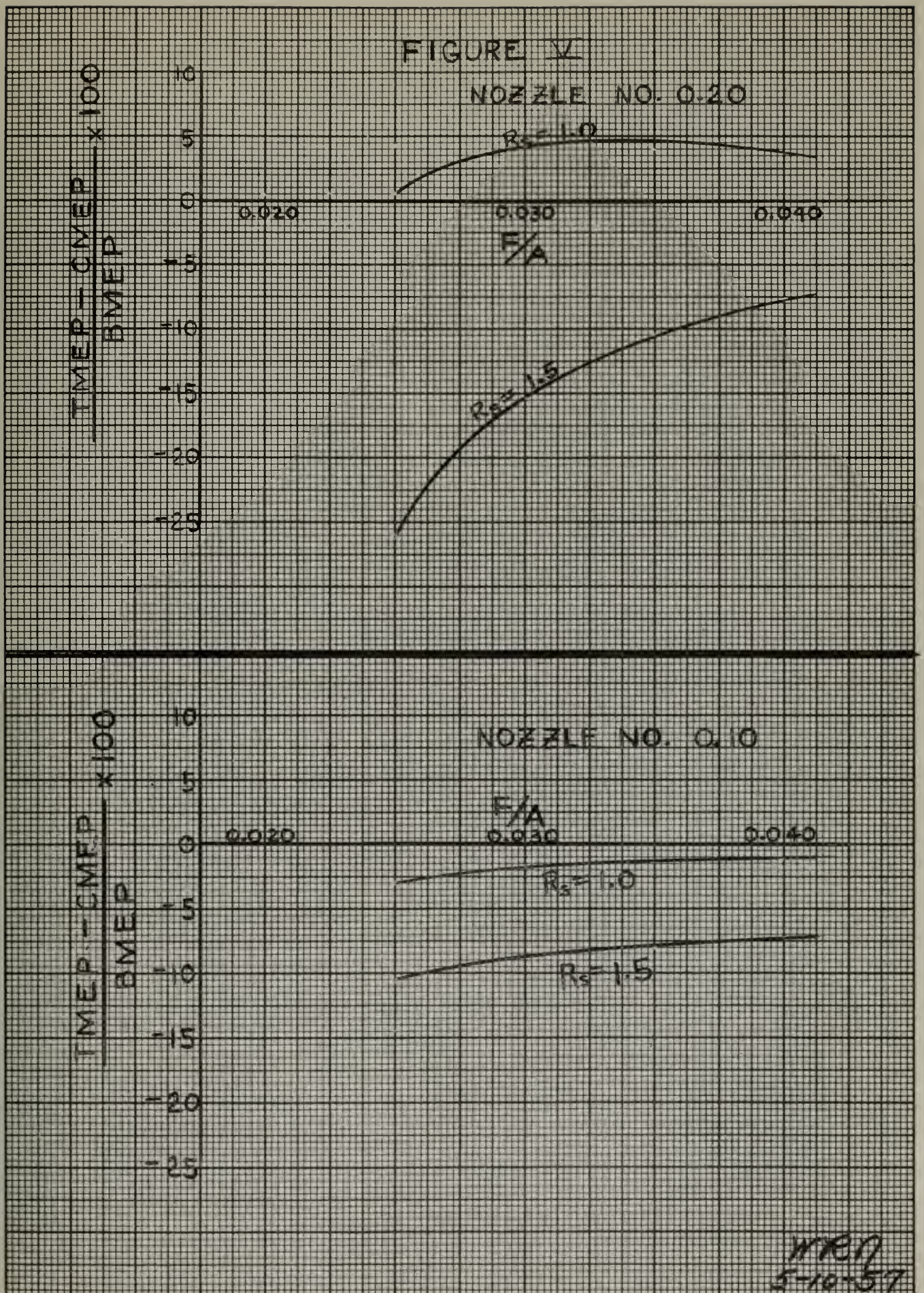
FIGURE V
NOZZLE NO. 0.20
R_s = 1.0
R_s = 1.5
F/A
0.020
0.030
0.040
10
5
0
-5
-10
-15
-20
-25
IMEP - CMEP / BMEP x 100
NOZZLE NO. 0.10
R_s = 1.0
R_s = 1.5
F/A
0.020
0.030
0.040
10
5
0
-5
-10
-15
-20
-25
IMEP - CMEP / BMEP x 100
WRN
5-10-57

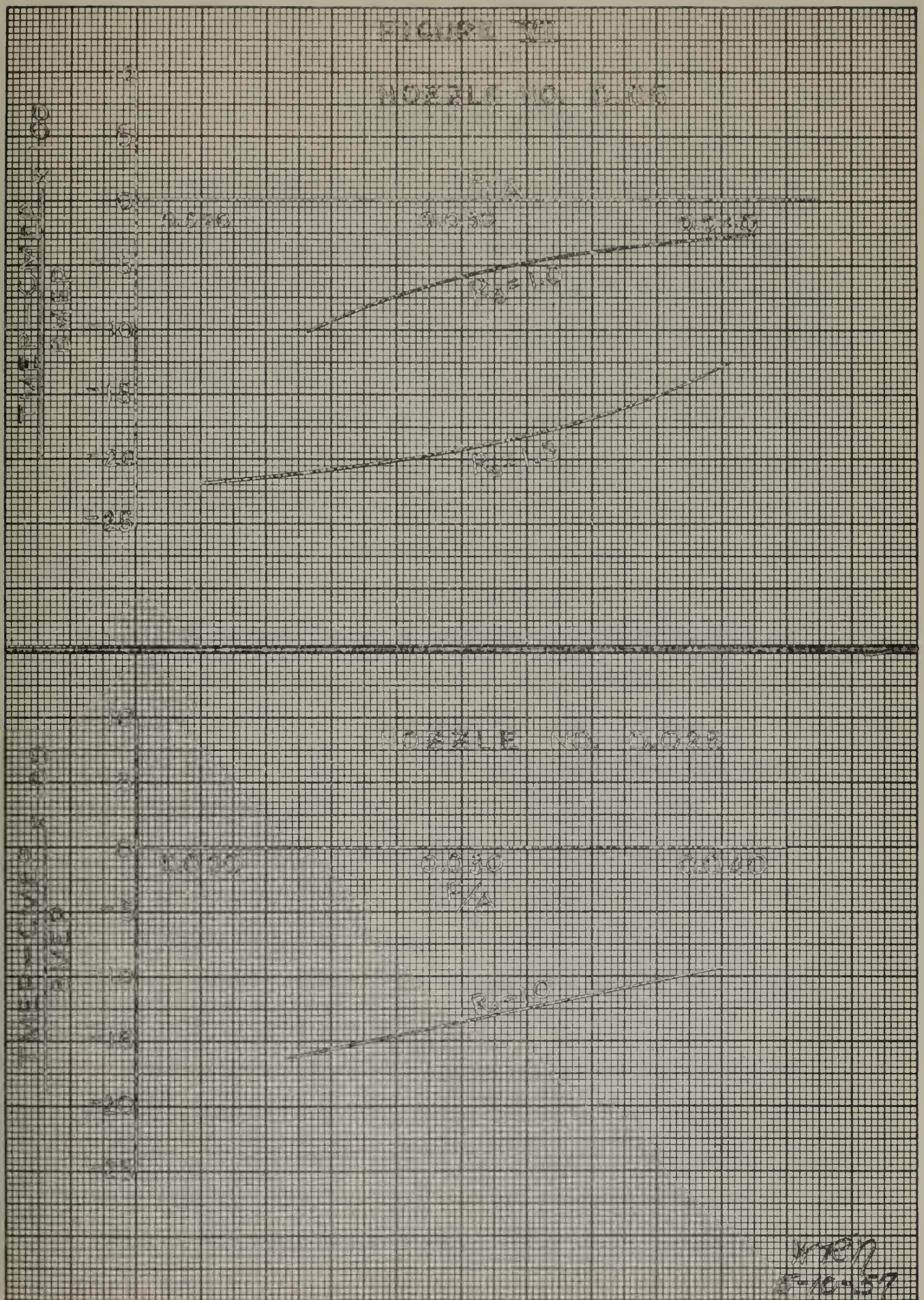

5-10-57

DISCUSSION OF RESULTS

The results presented above are influenced by the accuracy with which engine data can be taken, the errors introduced from friction estimates, and the possibility of error introduced through cross plotting techniques. The results are particularly sensitive to the cross plotting method employed. In reviewing the results and calculations, it was noted that the cross plotting for nozzle 0.05 was done with what appears to be poor judgement (see Figure XVIII). The curvature in the lines of constant R_S should have been omitted, as was done in the corresponding plots for the other three nozzles. If this change were to be made, it would eliminate the low point at F/A = 0.040, nozzle 0.05 in Figures I and II, resulting in the F/A = 0.040 line becoming almost a straight line, and in addition would eliminate the crossing of the BSFC curves of Figure IV.

From Figures V and VI, it is noted that under most conditions it is not possible to use a turbocharger alone on this engine. An engine driven or separately driven supercharger will be required in addition to the turbocharger. This is especially evident at the higher levels of supercharge which are attained when using the smaller nozzles. It is also noted that combined turbine-compressor work is a significant portion of net output.

The results expressed as net brake mean effective pressure as a function of nozzle area ratio, Figure II, shows that the level of supercharge is an inverse function of nozzle area. This is more evidence of the generally recognized fact that to supercharge a two-stroke engine, it is necessary to raise the exhaust pressure level. As exhaust pressure

is raised, scavenge density and cylinder air capacity increase. It appears that if there were some nozzle area at which the net BMEP vs. nozzle area curves could peak, it would be a nozzle area of very small size, implying mean pressures far in excess of those practicable. An examination of the BSFC curves reveals that there is an optimum value of nozzle area at about area ratio 0.10. The optimum is a significant one, with a BSFC decrease of about 10 per cent over neighboring nozzles. Because of the higher loading of the supercharged engine, we can expect the BSFC to be lower than that of the unsupercharged engine. This is verified by the rise in fuel consumption as nozzle size increases to the largest area ratio 0.20.

This study has examined but a very small part of an extensive field, and the interpretations made here are restricted to one set of piston speeds, valve timing and geometry, and compression ratio. The effects of these variables upon supercharged performance may be as great or even greater than the effect of nozzle area changes. The least difficult of these variables to study would be piston speed, as the identical study presented here could be repeated at 1200 and 2000 rpm (piston speeds of 1000 and 1670 fpm). From this study, the effects of piston speed changes could be analyzed.

In the design of unsupercharged engines, it is sometimes valuable to restrict exhaust port area, as a gain in trapping efficiency may be realized. However, when such an engine is turbocharged, the exhaust flow is restricted by the turbine nozzle, and the restriction of the exhaust ports produces a throttling of blow down which reduces the energy available for a turbine. In addition, restriction of exhaust valve area may also produce a high compressor work requirement if

substantially high scavenge ratios are to be maintained. The GM 3-71 diesel engine has a very low flow coefficient. In our work, this is reflected by the large compressor powers required as compared with the turbine work outputs. It would be well to examine the exhaust valve areas to determine if an area increase should be incorporated to improve the supercharged performance. Reference 1 indicates a method of engine gas flow analysis which probably can be expanded to an analysis of supercharged engine gas flow. Execution of this analysis could be a valuable guide as to changes which should be made, if any, in exhaust valve areas.

Finally, it appears that compression ratio should be seriously examined when considering supercharging an engine. The level of supercharge is limited by structural and thermal considerations, and these in turn are limited by total compression ratio, that is, supercharger and cylinder compression. The compression ratio of 17 of the test engine is quite high. When supercharged, net powers greater than rated power could be realized at lower compression ratios. While in reality this would probably increase fuel consumption, lower compression may be necessary in view of limitations of structural reliability. For these reasons it would be valuable to determine the effects of compression ratio upon optimum nozzle size.

CONCLUSIONS

1. In order to increase the output of two-stroke diesel engines by supercharging, it is necessary to increase the exhaust pressure.

2. There is an optimum nozzle-to-piston-area ratio of about 0.10, at which BSFC is a minimum.

3. It is impossible to supercharge this engine with a turbocharger alone. An engine driven or separately driven supercharger is necessary in addition to the turbocharger.

RECOMMENDATIONS

1. The work performed to date has been concerned only with engine performance at piston speed of 1335 fpm. Further work should be done to determine the effect of piston speed variations upon net engine performance as a function of exhaust nozzle area.

2. Brosens (1) presents a method of analysis for the scavenging process of two-stroke diesel engines. It is felt that this analysis could be expanded to include analysis of the scavenge process with exhaust nozzles fitted. Such an analysis would be a useful guide as to changes desireable in exhaust valve arrangements in order to improve supercharged performance.

3. Inasmuch as the level of supercharge is limited by peak pressure in the cylinder and by stresses in the engine, it appears desireable that the compression ratio of the engine be lower than the compression ratio of 17 of the unsupercharged engine. It appears desireable to examine the same engine operating at compression ratios as low as nine or ten, in order to determine the effect of compression ratio upon the choice of exhaust nozzle area.

APPENDICES

APPENDIX A

THE USE OF A FLAT PLATE TO MEASURE THE WORK A TURBINE COULD REMOVE FROM A CYCLIC JET FLOW

Development of Equations

In work on the use of internal combustion engine exhaust energy, it is common to use the thrust felt by a flat plate, perpendicular to the exhaust, as a measure of the work which a turbine could remove from the exhaust stream. The following analysis shows the basis of the method.

Figure VII

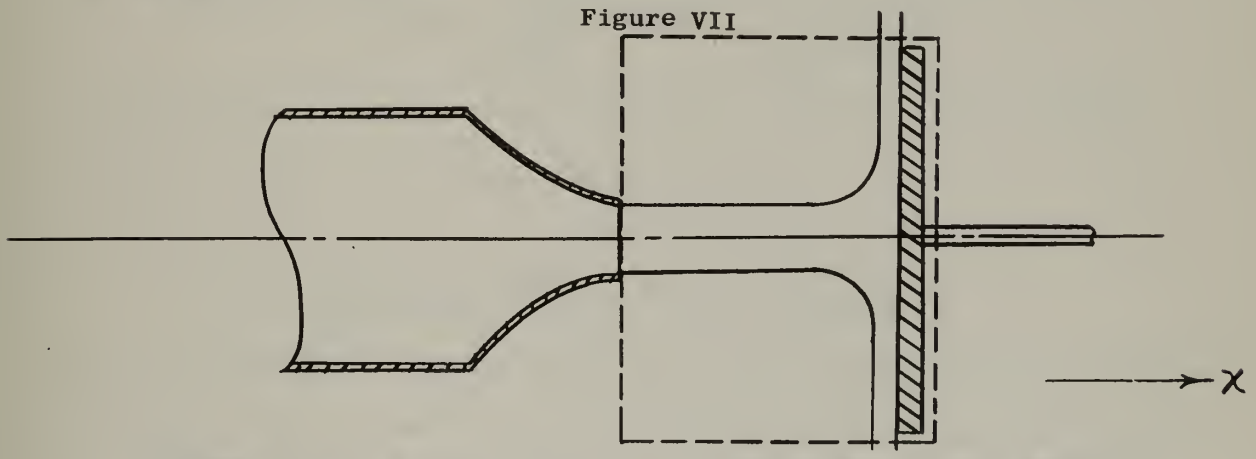

Assume we have a nozzle with a jet issuing from it and impinging upon an infinite plane, perpendicular to the axis of the nozzle. Let us draw a control surface consisting of a plane perpendicular to the nozzle axis at the nozzle throat, a plane perpendicular to the nozzle axis and behind the deflecting plane, and a cylindrical surface connecting the two planes, at such a distance from the nozzle axis so that the flow crossing it is perpendicular to the nozzle axis. The control volume is the volume contained within this control surface.

Letting x represent the axial direction as indicated, the momentum equation for the control volume can be written as:

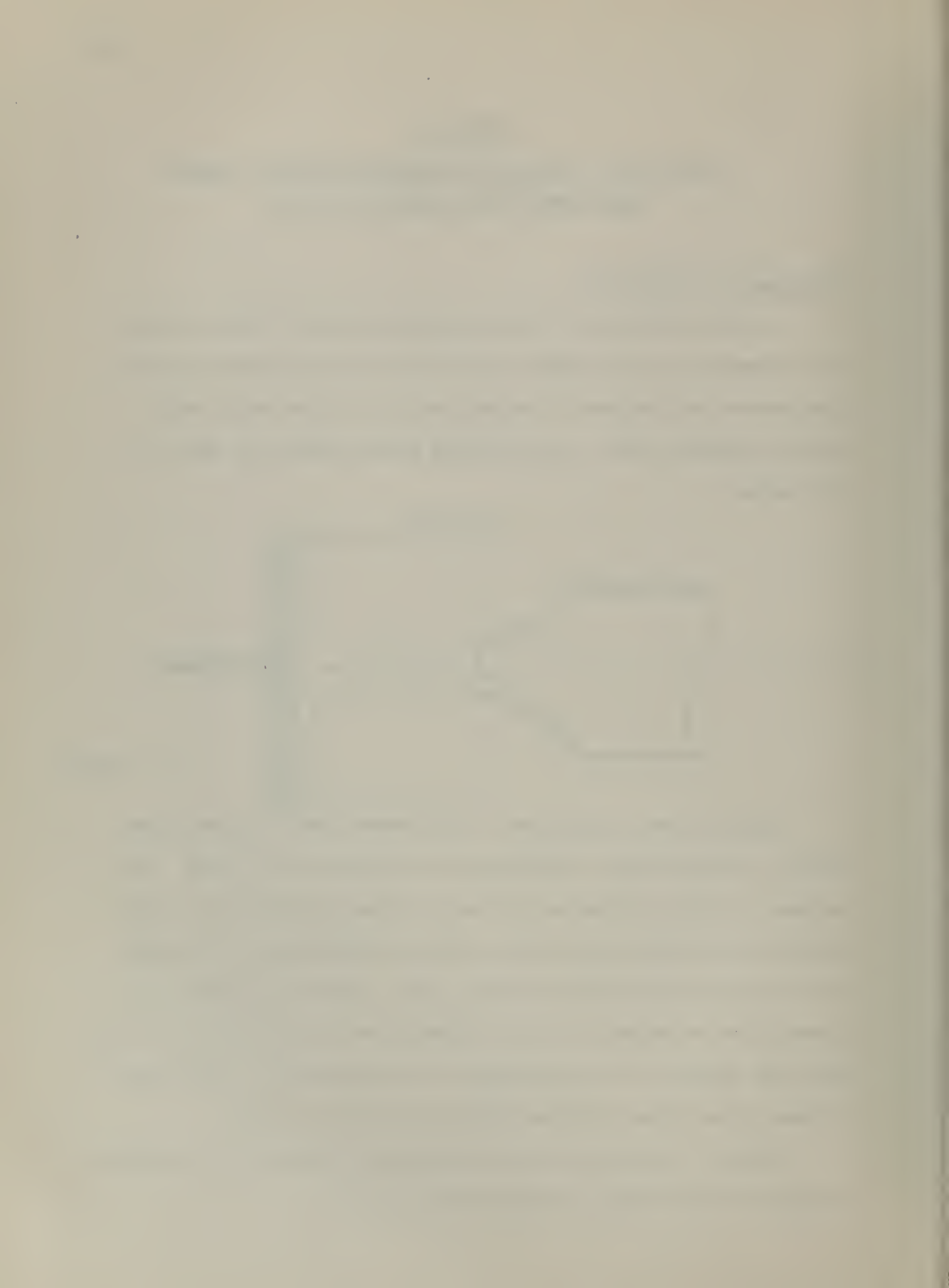

$$F_x = \int_{VOL} \frac{\partial}{\partial t}(\rho V_x)\, d\mathcal{V} - \int_A \rho V_x^2\, dA$$

Where F_x is the external force applied to the control volume, ρ is the density of the fluid of the jet, V_x is the velocity in the x direction and the area and volume integrals are taken over the control surface or volume.

If the pressure in the nozzle throat is p_t, and everywhere else on the control surface the pressure is p, and if we let the external force applied to hold the plate be F:

$$-F + (P_T - P)A_N = \int_{VOL} \frac{\partial}{\partial t}(\rho V_x)\, d\mathcal{V} - \int_A \rho V_x^2\, dA$$

If we assume the flow is one-dimensional so that the flow is uniform across the nozzle, then at any instant of time:

$$-F = \int_{VOL} \frac{\partial}{\partial t}(\rho V_x)\, d\mathcal{V} + [P - P_T - \rho V_x^2]A_N$$

Let us integrate this instantaneous force over the period from t_1 to t_2, and let us define a mean force, $\bar{F}$, as the time mean of the force. We then obtain:

$$-\bar{F} = \frac{1}{t_2 - t_1}\int_{VOL} \rho V_x\, d\mathcal{V}\Big]_{t_1}^{t_2} + \frac{1}{t_2 - t_1}\int_{t_1}^{t_2} (P - P_T - \rho V_x^2)A_N\, dt$$

If the jet flow is cyclic in time, and t_1 and t_2 correspond to identical points in the cycle, the first integral becomes zero, and we have as our final result:

$$\bar{F} = \frac{1}{t_2 - t_1}\int_{t_1}^{t_2} (P_t - P)A_N\, dt + \frac{1}{t_2 - t_1}\int_{t_1}^{t_2} \rho V_x^2 A_N\, dt \qquad \text{.....(1)}$$

Let us now consider an ideal impulse turbine with "zero angle" blades--that is, the gas velocities are all assumed in the tangential direction and axial velocities are assumed negligible. If we let the absolute velocity leaving the nozzle be represented by C_1, and the wheel speed by U, the relative velocity entering the buckets by w_1, the relative leaving velocity by w_2, we obtain a velocity diagram as follows.

Figure VIII

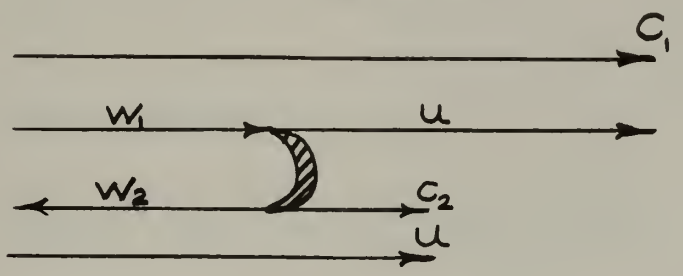

The force in the tangential direction is given by:

$$F_t = \dot{m}(w_1 - w_2) = \dot{m}(2w_1) = 2\dot{m}(C_1 - u)$$

Where $\dot{m}$ represents the mass rate of flow per unit time.

The element of work done per differential element of time is then:

$$dW = 2\dot{m}(C_1 - u)u\,dt$$

And, if the flow is cyclic, the work done per cycle is:

$$W_{CYCLE} = \int_{t_1}^{t_2} 2\dot{m}(C_1 - u)u\,dt = 2u\int_{t_1}^{t_2} \dot{m}C_1\,dt - 2u^2\int_{t_1}^{t_2} \dot{m}\,dt$$

The mass rate of flow can be found by integrating the flow over the exit plane of the nozzle, which becomes with a one-dimensional assumption:

$$\dot{m} = \rho C_1 A_N$$

This then leads to an equation forthe work per cycle:

$$W_{CYCLE} = \int_{t_1}^{t_2} 2u\rho C_1^2 A_N \, dt - 2u^2 \int_{t_1}^{t_2} \dot{m} \, dt \qquad \text{.....(2)}$$

Comparing this with equation (1), we can see for the special case where the nozzle is unchoked (p_t = p):

$$W_{CYCLE} = 2u\bar{F}(t_2 - t_1) - 2u^2 \int_{t_1}^{t_2} \dot{m} \, dt$$

And then the power becomes:

$$P = 2u\bar{F} - 2u^2\dot{M} \qquad \dot{M} = \frac{\int_{t_1}^{t_2} \dot{m} \, dt}{(t_2 - t_1)}$$

Differentiating the above expression with respect to the wheel speed, and setting the derivative equal to zero gives the value of wheel speed for maximum power. Substituting this back in our equation for power, we obtain the maximum obtainable power:

$$P = \frac{\bar{F}^2}{2\dot{M}} \qquad \text{.....(3)}$$

In the case where the nozzle is choked for a portion of the cycle, the analysis presented above may be in error. It becomes necessary to make some further assumptions about the flow within the turbine. If we assume that the turbine nozzle expands the jet to the critical velocity, and the drop to exhaust pressure does not take place until after the fluid has left the turbine rotor, the formula above will indicate

a turbine power which is too large, due to the pressure difference terms measured by the force plate, and indicated in equation (1). If, on the other hand, we assume that after the gas leaves the nozzle and before it enters the turbine wheel the pressure drops and the velocity increases so that jet pressure is equal to surrounding static pressure, the analysis as presented above will still be correct.

The true behavior of the turbine is probably somewhere between these two assumptions. Therefore, the error in turbine work prediction by this means should be less than the error arising in the first assumption--the error due to the mean pressure difference between static pressure at exhaust and the nozzle throat pressure.

Development of a Force Measuring Device, General

It was desired that the diesel exhaust gas be kept contained, and not be allowed free escape into the testing laboratory. For this reason, the jet deflecting plate was placed within the exhaust gas receiver, a tank of approximately eighteen inches diameter and three-foot length. The exhaust nozzles terminated just within this tank, and there was ample room to permit the installation within the tank of a deflecting plate of six-inch diameter, which was deemed adequate for the purpose. Mean forces of about five or six pounds maximum were anticipated, and it was necessary to devise a method of measuring these forces.

The deflecting plate was mounted on a small cantilever beam, and electrical resistance strain gauges were employed to determine the force which was exerted by the jet. While the strain gauge method involved additional problems of cooling (the gauges had to be water cooled) and the need for additional equipment such as strain gauge indicators, the method provided a good solution to the problem of reading a force within the exhaust tank.

Development of a Force Measuring Device: Strain Gauge Circuitry

Strain gauge circuits have been designed which permit the direct measurement of shear in a beam, and one such circuit was employed for this purpose. (Ref. 6) Figures IX and X show the arrangement of the cantilever beam and force plate and the strain gauge arrangement and circuitry. The advantage of the strain gauge arrangement shown is that it produces a strain reading proportional to the shear force in the beam, regardless of the point of application of the force, as long as this point is not between the gauges A and B. In addition, any moment or axial forces applied to the beam do not produce a strain reading. Finally, if the temperature along the bar is not uniform, but is only a function of the axial position along the bar, the bridge arrangement compensates for the temperature differences.

These characteristics can be shown as follows. Let us assume that the beam has uniform rectangular cross section. This means a constant section modulus and a neutral axis equidistant from the upper and lower surfaces on which the strain gauges are mounted. Let us assume for the moment that with no force acting and uniform temperature along the bar, all strain gauges have equal resistance, R. Let the change in resistance due to strain be $(\epsilon R)_A$, $(\epsilon R)_B$, $(\epsilon R)_C$, and $(\epsilon R)_D$; and the changes in resistance due to temperature changes be $(\Delta TR)_A$, $(\Delta TR)_B$, $(\Delta TR)_C$, and $(\Delta TR)_D$. It can be shown that for a bridge circuit of this type:

$$\text{Output} \propto R_B R_C - R_D R_A$$

$$\text{Output} \propto \left[R + (\epsilon R)_B + (\Delta TR)_B\right]\left[R + (\epsilon R)_C + (\Delta TR)_C\right] - \left[R + (\epsilon R)_A + (\Delta TR)_A\right]\left[R + (\epsilon R_D) + \Delta TR)_D\right]$$

Figure IX

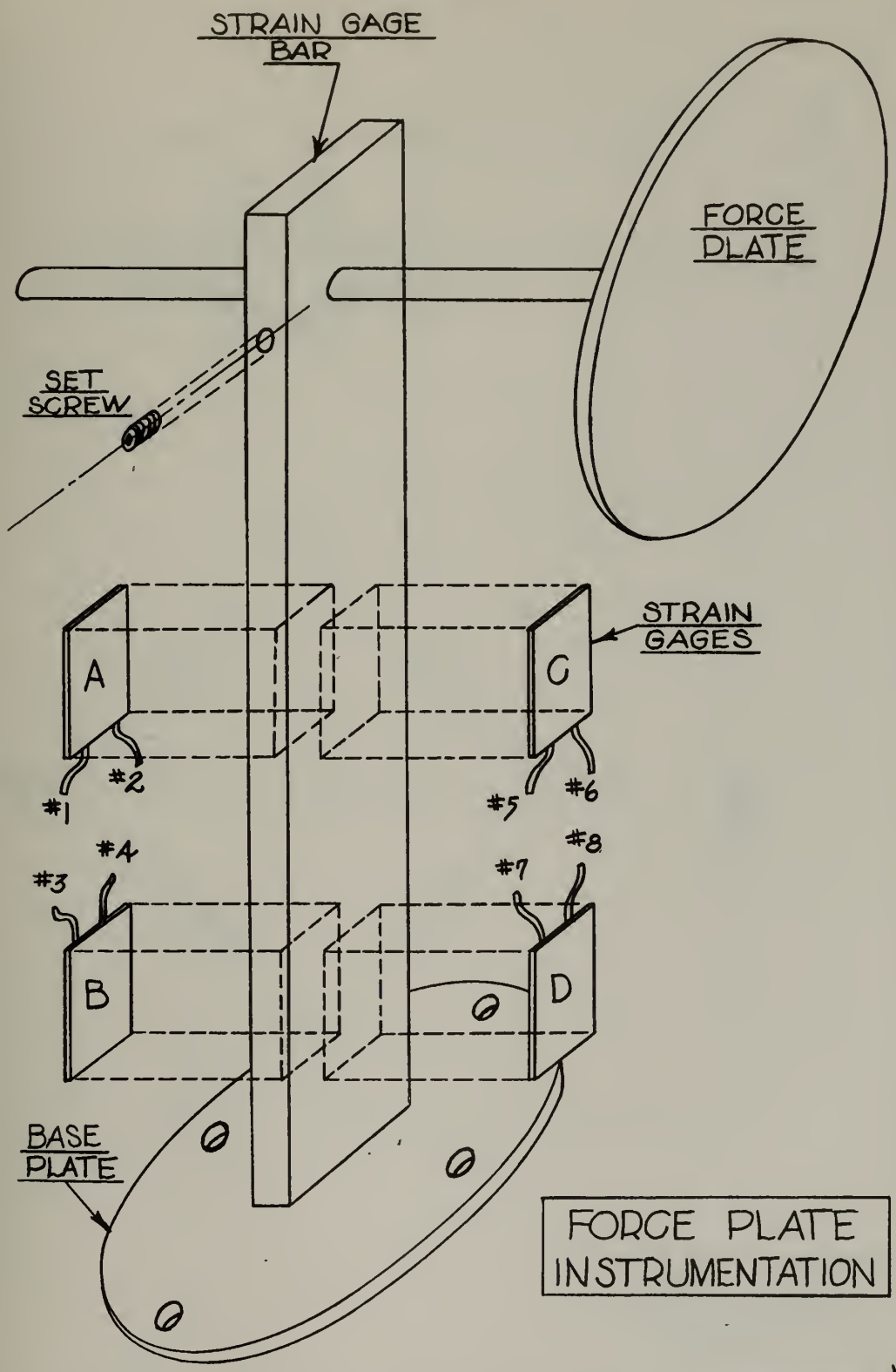
STRAIN GAGE BAR
FORCE PLATE
SET SCREW
STRAIN GAGES
A
B
C
D
#1
#2
#3
#4
#5
#6
#7
#8
BASE PLATE
FORCE PLATE INSTRUMENTATION
5-10-57 dhg

Figure X

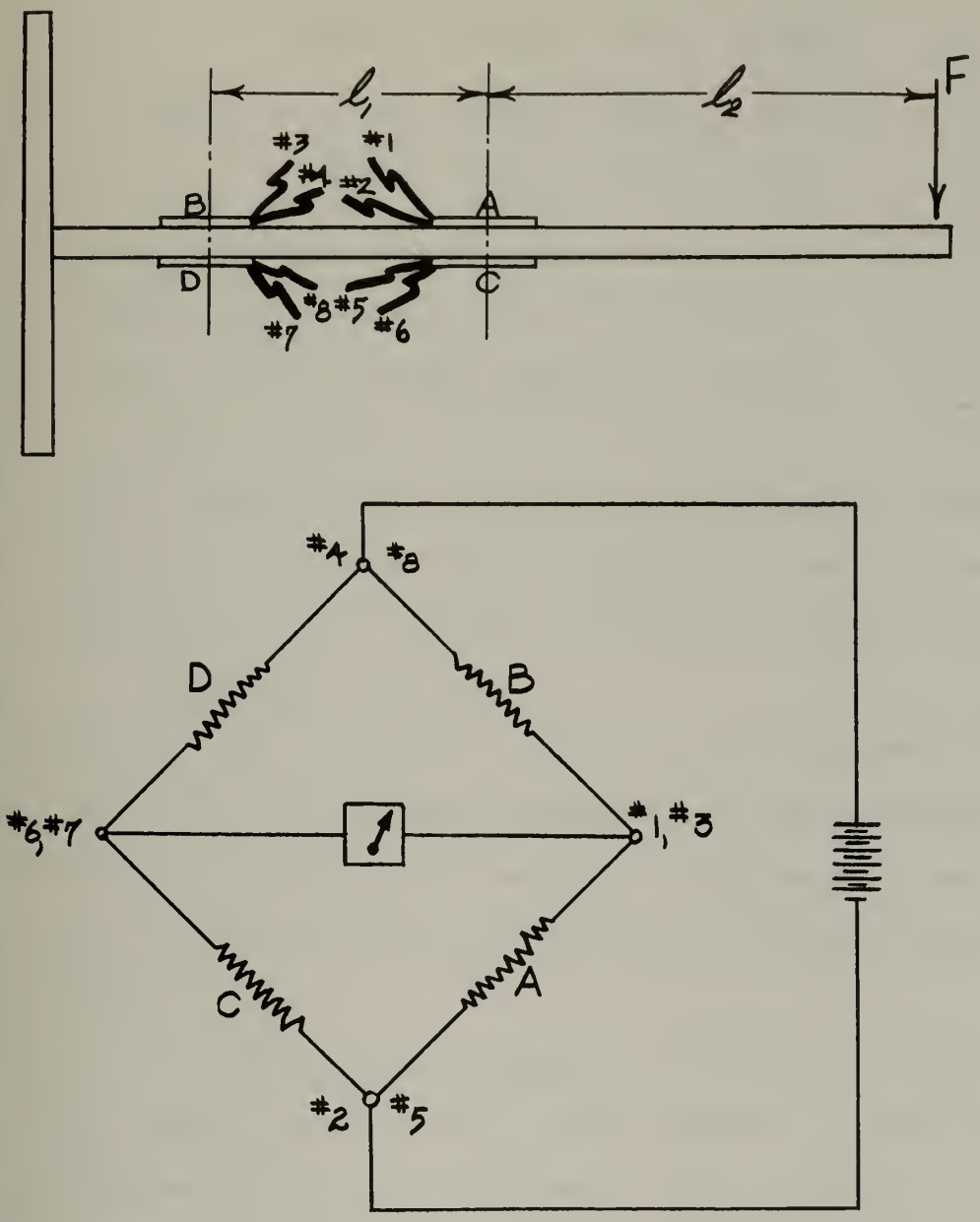

STRAIN GAGE CIRCUIT

5-10-57 drg

Expanding and dropping higher order differentials:

$$\text{Output} \propto (\epsilon R)_C + (\Delta TR)_C + (\epsilon R)_B + (\Delta TR)_B - \left[(\epsilon R)_A + (\Delta TR)_A + (\epsilon R)_D + (\Delta TR)_D\right]$$

$$\text{Output} \propto (\epsilon R)_B - (\epsilon R_D) - \left[(\epsilon R)_A - (\epsilon R)_C\right] + (\Delta TR)_C - (\Delta TR)_A + (\Delta TR)_B - (\Delta TR)_D$$

If the temperature is a function of axial position only, the temperatures will be the same at A and C, and the same at B and D. This means there is no portion of the output due to temperature variations.

If we consider for a moment only the force F acting on the beam, we see that at B and D, the strain is proportional to the moment $F(l_1 + l_2)$, while at the gauges A and C, the strain is proportional to the moment Fl_2. For this case, the output is proportional to:

$$(Fl_1 + Fl_2) - Fl_2 = Fl_1$$

Since l_1 is a constant of construction, and l_2 disappears from our expression, the strain gauge arrangement will give a reading proportional to the force regardless of the point of application of the force. (Note that this is true only if the force is not applied between the pairs of gauges.)

If a bending moment is applied to the end of the beam, it will produce identical strains at each set of gauges. If a direct tension or compression is applied to the beam, it will also produce identical strains at each set of gauges. Thus, the arrangement will produce an output proportional to shear regardless of other moments or direct stresses applied to the beam.

By the use of this circuit, it was not necessary to know precisely the center of impact of the gas jet on the force plate, nor to be

concerned if the force plate applied a moment as well as a force to the cantilever. As the bar was water cooled, with the heat input coming from the force plate at the upper end, a temperature variation along the bar was certain, and the temperature compensating feature of the circuit was essential. As considerable stability was desired, bakelite strain gauges were employed (SR-4, Type AB-1).

Development of the Force Measuring Device: Strain Gauge Waterproofing

As the bar was to be water cooled, it was necessary to waterproof the strain gauges and associated wiring. The most recent recommendations from the Baldwin-Lima-Hamilton Company are based upon U. S. Naval experience, and suggest the use of a polysulfide synthetic rubber compound for waterproofing and protecting strain gauges (Ref. 2). In this experiment, Minnesota Manufacturing and Mining synthetic rubber compound EC 801 was employed. If the manufacturer's instructions are carefully followed, it was found to be easy to apply and successful in operation. A number of suggestions with regard to waterproofing this type of arrangement are:

1. Be certain that all metallic surfaces to which the polysulfide must bond are clean of any rust, scale or oil or grease film. A final washing with acetone prior to application of the waterproofing compound is recommended.

2. The greatest difficulty in waterproofing occurs due to the electrical leads. These must penetrate the waterproof layer, and there is good chance of water entry along the leads if care is not used. In this regard, during the wiring of the gauges, one should bear in mind that waterprooding will follow. This indicates that leads will be arranged so that access to the bare metallic portions of leads and to

strain gauges is easy, and that lead arrangements which will present obstacles in placing the waterproofing compound in place must be avoided.

3. Successful waterproofing is not dependent upon a thick coat of compound, although several layers may be found necessary. Our experience indicates that great care must be exercised in applying the first coat. It is essential that good bonding occurs between the metallic leads and the rubber compound, and that a layer of the compound is built up between the leads and the metal bar. Successive coats cannot correct a deficiency in this regard.

Development of the Force Measuring Device--Mechanical Design

If the cantilever bar-force plate combination is to read the average force, it is necessary that the natural period of the bar be long when compared with the period of exciting forces to which it is subject. The lowest frequency component of the force applied to the bar is the frequency of the engine exhaust pulses--in our case of one-cylinder operation, the rpm of the engine. In addition to the frequency question, it is desireable to have large strains in the bar so that the strain gauge system can develop its full accuracy. Both of these items suggest a very flexible cantilever.

On the other hand, there are two arguments for using a stiff cantilever. First, it is desired that the force plate remain fairly close to the nozzle and not have very large movements from its rest position. Second, the arrangement employed was water cooled by enclosing the cantilever in a pipe, perforated at the upper end and so arranged that a running water level was maintained at a height of a few inches above the upper strain gauge. Large deflections would bring the cantilever

into contact with this pipe and obviously produce erroneous reading of jet force.

The final design employed a cantilever of dimensions 3/16" x 3/4" x 16", with strain gauges located on 9-in. centers. This was quite successful for operation at 1600 rpm, the natural period of the bar being below 400vpm. The maximum deflection of the bar permitted by the pipe was about one inch, and required a force of about seven pounds. This very nicely covered the engine operating range at 1600 rpm. At 2000 rpm, where larger forces will be encountered, a larger bar is indicated.

Operating Experience with the Force Measuring Device

The bar was calibrated by applying known forces to the plate and a scale factor was determined. Using a Baldwin-Lima-Hamilton Type M strain indicator, this factor was 140 micro-inches per inch per pound force. As anticipated, the bar was found insensitive to moments applied. In use, with the scale factor of 140, it is estimated that the strain gauge technique gave accuracy of within 0.05 pounds of the mean force felt by the force plate. The device was very easy and quick to read and employ. Zero readings were checked at the start of each run and were found to be stable.

After Run 133, at which time the force plate had been used with the engine operating for more than twenty hours, the zero of the force bar was found to have changed. The check of resistance to ground indicated that a ground had appeared in the circuit, so the bar was removed and waterproofing was repeated. Upon recalibration of the bar after this second waterproofing, it was found that the scaling factor had increased to about 170 micro-inches per inch per pound, and that the bar was now very sensitive to the point of application of the force. Both the

increase of the scaling factor and the lack of compensation for moments indicate that either gauge A or gauge C had lost its bond to the cantilever and was not being fully strained as the bar deflected. The effect of this would be as noted above. During the removal of the bar for waterproofing, it had received fairly severe handling, and it is not certain if the bond failure had occurred during this removal or at some earlier time. The remainder of the test runs employed the nozzle analysis and force integration method indicated below to determine turbine power.

Conclusions Regarding Strain Gauge Application to Force Plate Measurement

While the failure of this device after about only twenty-five engine operating hours could indicate a lack of structural reliability of devices of this type, the experimenters believe that the device is highly useful in this application, and can be made durable enough to warrant continued use. The strain gauges applied here were the first that these persons had mounted, and it is not surprising that the bond of one of these gauges would have failed. The strain gauge method provides a means of carrying information out of the exhaust tank with minimum requirements for openings in the tank, and effectively no leakage of exhaust gas into the laboratory. Once manufactured, the device is very simple to use and can be arranged so that calibration checks are quick and easy. Its further development and employment is recommended.

Comparison of Force Plate Readings and Predicted Values from Exhaust Pipe Pressures

From the analysis of the force plate, it was shown that the force due to momentum change can be expressed as:

$$F' = \rho V_x^2 A_N$$

Using the relations for isentropic, one dimensional flow, this can be shown to be:

$$F' = \left(\frac{2K}{K-1}\right) P_t A_N \left[\left(\frac{P_o}{P_t}\right)^{\frac{K-1}{K}} - 1\right]$$

Where F' is the instantaneous force due to momentum change

k is the ratio of specific heats

p_t is the pressure at the nozzle throat

p_o is the stagnation pressure at the nozzle

A_N is the nozzle throat area.

The total force exerted on the plate would then be:

$$F = F' + (p_t - p)A_N$$

Where p is the pressure outside the nozzle.

Data taken for the runs included stagnation pressures as a function of crank angle at a point just ahead of the nozzle. From these pressures and the measured pressure in the exhaust tank, instantaneous forces could be computed, and graphed as a function of crank angle. These curves could then be mechanically integrated, and the mean force thus determined.

Figure XI is a plot of the pressure ratio across the nozzle (P_o/p) and of the instantaneous computed force as functions of crank angle.

Figure XXV is a graph of the term $\left(\frac{P_A}{P_D}\right)^{\beta} - 1$ which was used for the computations. A value of k = 1.363 was chosen which was a good mean value for diesel exhaust composition at the mean exhaust temperatures.

After the strain gauge had become defective, this method of determining mean force was used for all runs (runs 134-152). Table II shows the variation between force plate readings and computed force for a variety of runs.

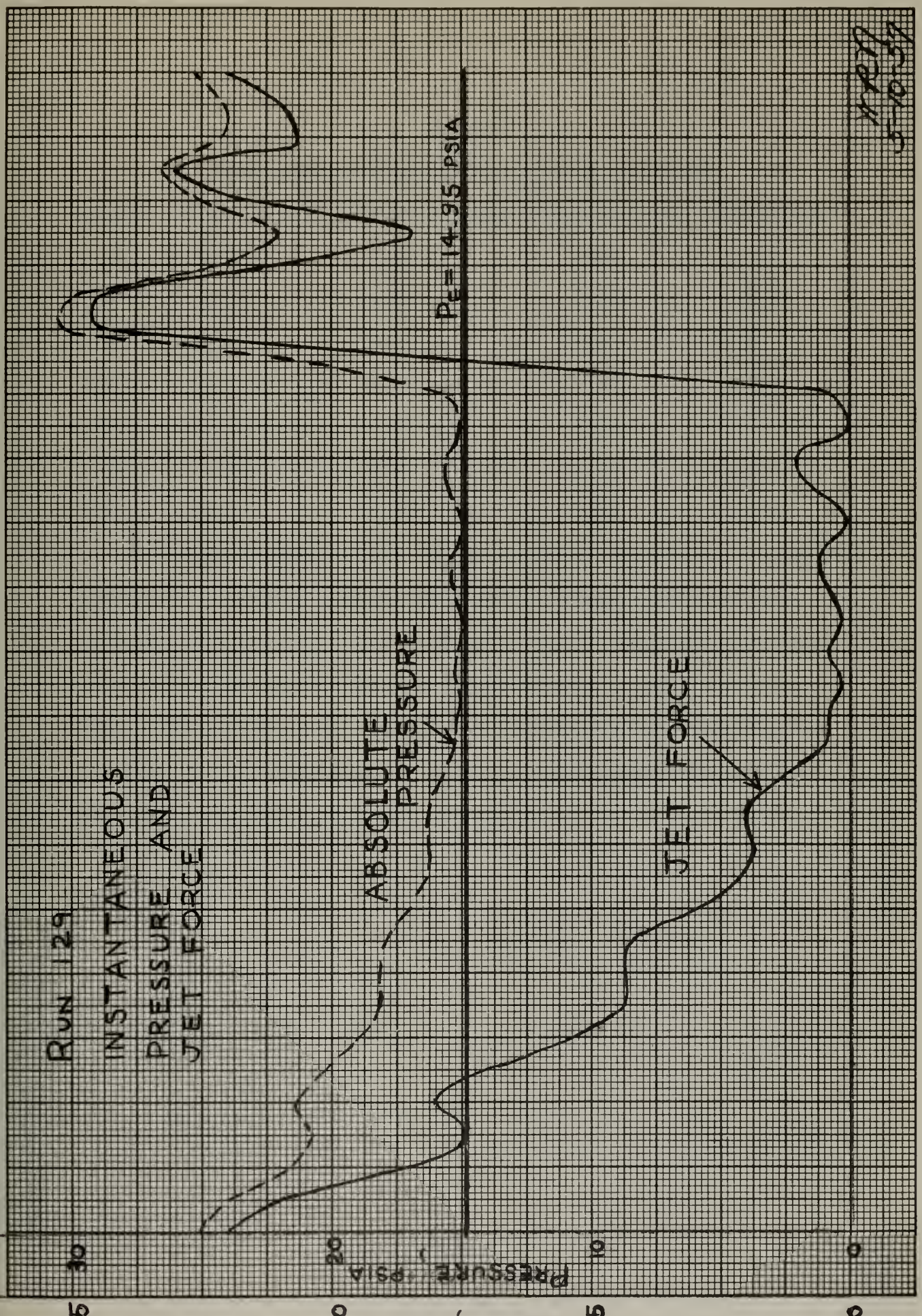
RUN 129
INSTANTANEOUS PRESSURE AND JET FORCE
ABSOLUTE PRESSURE
JET FORCE
P_e = 14.95 PSIA
PRESSURE, PSIA
FORCE, LBS
20
15
10
5
0

Figure XI

TABLE II

COMPARISON OF COMPUTED AND MEASURED JET FORCES

Run No.	Nozzle No.	Force Plate Reading	Computed Force	% Difference
10	0.20	3.03 lb	2.89	- 4.6
25	0.025	4.95	4.42	-10.7
125	0.10	4.14	5.63	+36.
128	0.05	7.11	7.20	+ 1.3
129	0.05	5.35	5.29	- 1.1
130	0.05	5.78	4.96	-14.5
131	0.05	3.64	3.16	-13.2

The pressure card for run 125 was questioned by the authors, as it indicated a very slow pressure decay in the exhaust pipe after blow down was completed. This may indicate an error in indicator operation at this run, and explain the high computed value of force from this card. The differences of the order of ten per cent occurring for the remainder of the comparison are deemed quite reasonable for measurements made with engine pressure indicators.

APPENDIX B

DETAILS OF PROCEDURE

Experimental Setup

1. Engine arrangement.

A GM 3-71 engine was used with one active cylinder:

Bore: 4.25 in.

Stroke: 5.00 in.

Compression ratio: 17

RPM (rated): 1600

An exhaust pipe took off from the exhaust manifold of the active cylinder. One firing cylinder of this engine was used so as to credit all measurements and effects accurately on a one-cylinder basis. The two inactive cylinders had their exhaust manifolds blanked off and were disconnected from the fuel racks. A compression process in which the compression work was balanced almost entirely by the expansion work resulted from the normal functioning of the intake air ports. It was assumed that the only contributing effect then of the two inactive cylinders to the experimental investigation was an addition to the friction horsepower. A brake load dynamometer was connected to the engine.

The majority of test runs was made with a standard 80mm injector. It was discovered that high fuel-air ratios could not be attained during supercharged operation at high scavenging ratios. A special 100mm injector was therefore installed which enabled the full range of fuel-air ratios to be obtained during supercharged operations at high scavenging ratios.

Figure XII

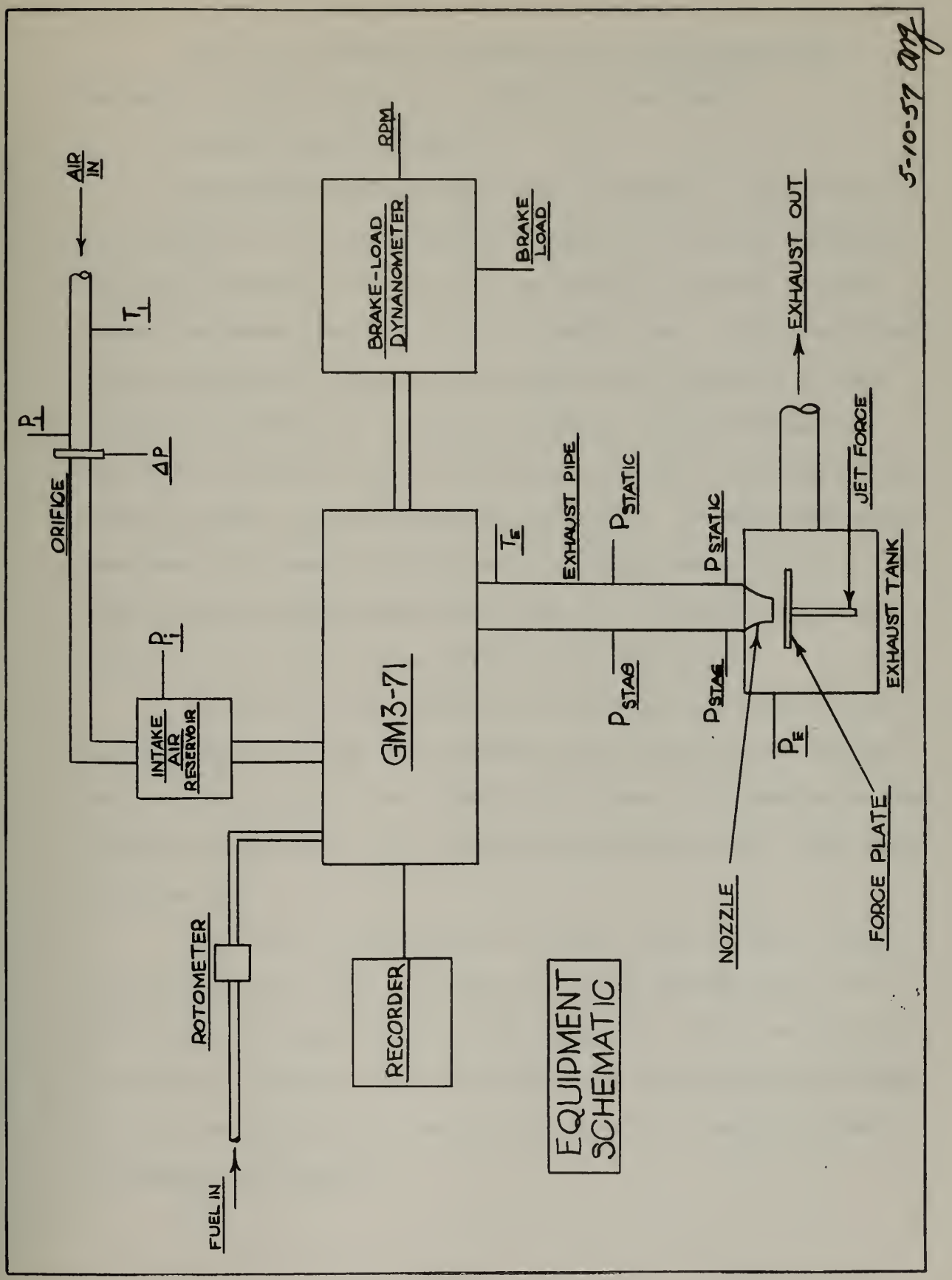
AIR IN
T_1
P_1
ΔP
ORIFICE
INTAKE AIR RESERVOIR
P_i
GM3-71
RPM
BRAKE-LOAD DYNANOMETER
BRAKE LOAD
T_E
EXHAUST PIPE
P_{STATIC}
P_{STAG}
P_{STATIC}
P_{STAG}
P_E
EXHAUST OUT
JET FORCE
EXHAUST TANK
NOZZLE
FORCE PLATE
ROTOMETER
RECORDER
FUEL IN
EQUIPMENT SCHEMATIC
5-10-57

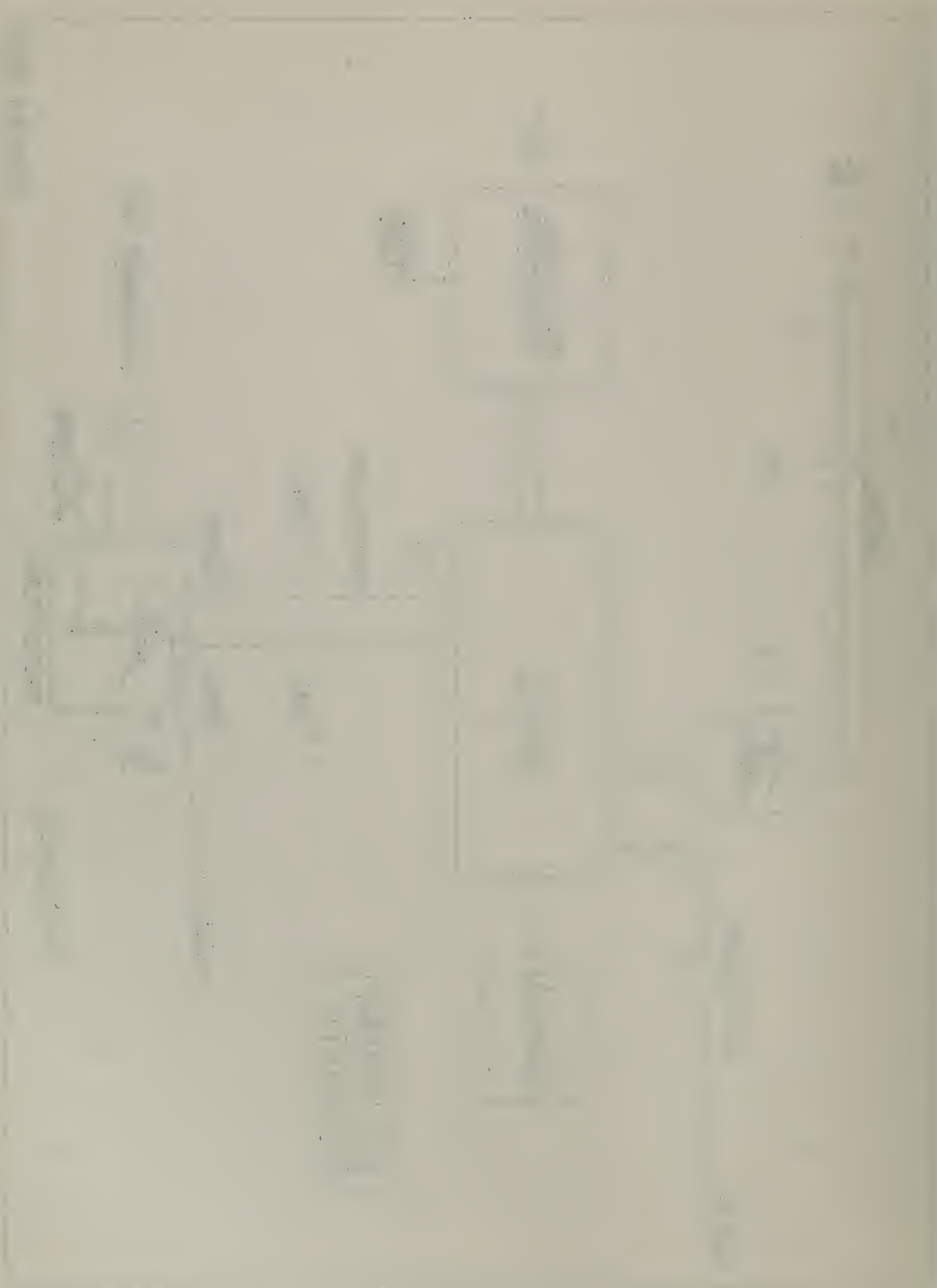

The M.I.T. Balanced Diaphragm Pressure Pickup was used to determine cylinder pressure as a function of crank angle.

2. Exhaust pipe arrangement.

Figure XIII shows the exhaust pipe arrangement. Essentially it is a 2-3/4-in. I.D. steel pipe which connects with the port opening of the active cylinder. This pipe size was chosen to minimize the area change from exhaust manifold port into exhaust pipe. A shielded thermocouple was placed in the pipe at the engine end to record an average exhaust gas temperature. At the mid-length of the pipe and again at the end of the pipe as close to the nozzle as possible were placed two pressure pickups, one static and one stagnation. Indicator cards made from these four pressure pickups gave a pressure-time variation in the pipe. These pressure pickups were of the M.I.T. Balanced Diaphragm type. The L/D ratio of the stagnation probes used was 12.

At the end of the exhaust pipe were placed the nozzles. The nozzle parameter (called nozzle number) used to describe them was the ratio of nozzle throat area to engine piston area. For geometry of the nozzles see Figure XIV. Four different nozzles were used: 0.025, 0.05, 0.10, and 0.20.

The nozzle discharges into an exhaust tank receiver in which is mounted a force plate. This plate is placed perpendicular to the gas flow approximately 1-1/2 in. from the nozzle. The force plate is mounted on a cantilever beam, and strain gages are employed to determine the force necessary to hold the plate in place. For details of this arrangement see Appendix A.

Figure XIII

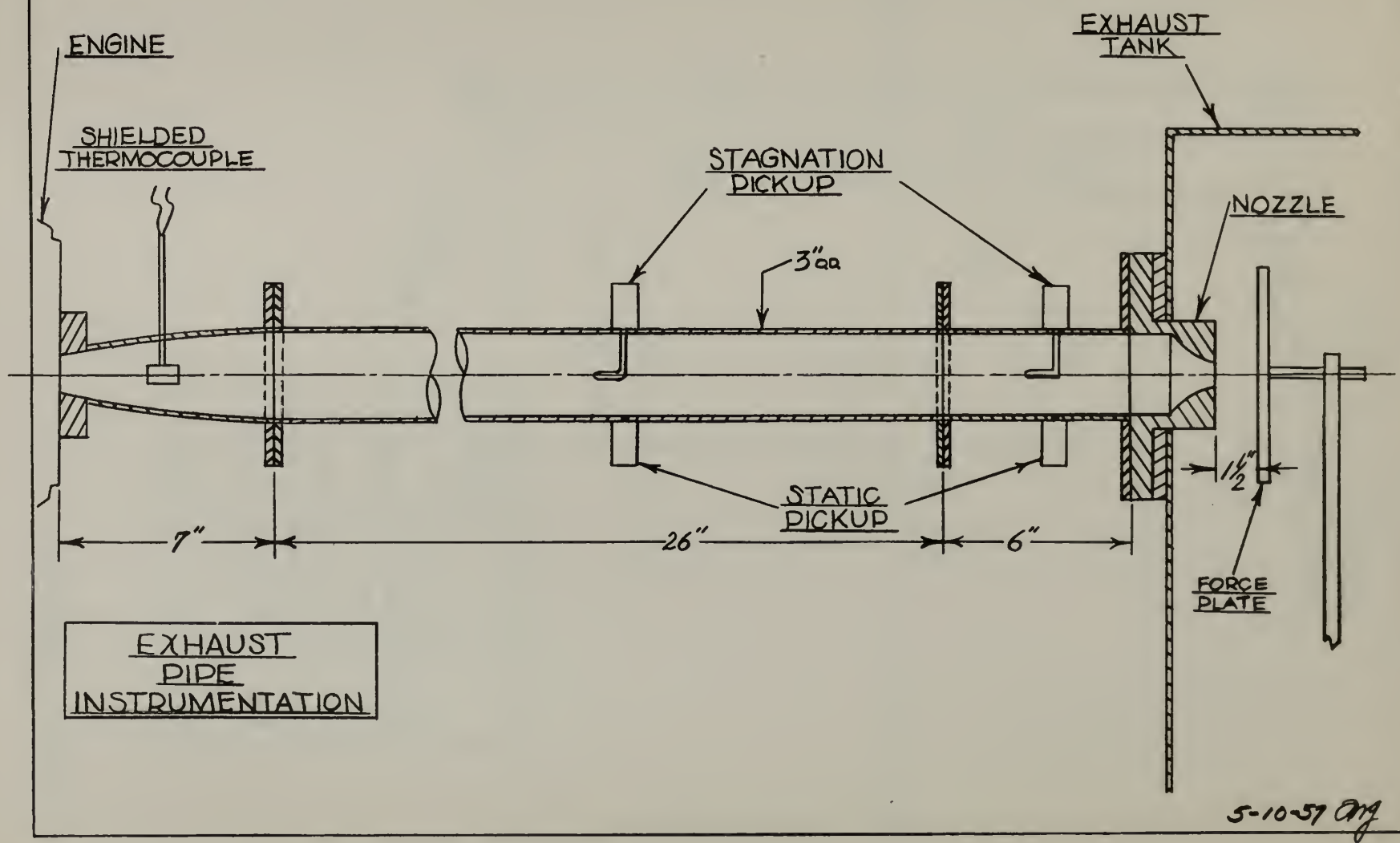
ENGINE
SHIELDED THERMOCOUPLE
STAGNATION PICKUP
3" OD
EXHAUST TANK
NOZZLE
STATIC PICKUP
1½"
FORCE PLATE
7"
26"
6"
EXHAUST PIPE INSTRUMENTATION
5-10-57

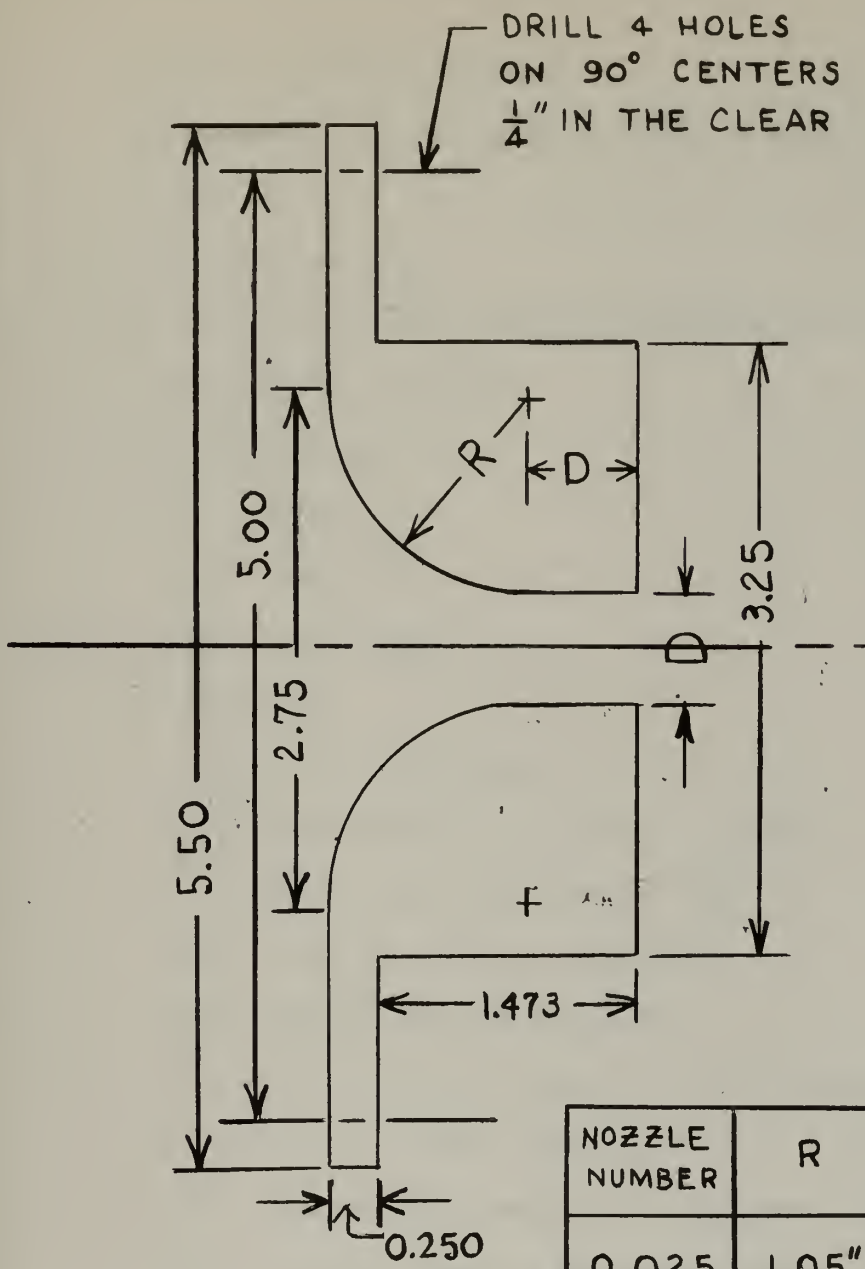

NOZZLE NUMBER	R	D
0.025	1.05"	0.673
0.050	1.00"	0.953
0.100	0.94	1.344
0.200	1.25	1.906

5-10-57 WRN

3. Summary of recorded readings.

The following recorded data was taken at each run:

a. RPM

b. Brake load ("H_G)

c. Force plate (microinches, allowing direct conversion to mean force in pounds).

d. Temperatures (°F)

(1) Exhaust gas

(2) Inlet air

(3) Water jacket

e. Pressures

(1) Oil pressure (psi)

(2) Air before inlet orifice ("H_G gage)

(3) Air across inlet orifice ("H_2O)

(4) Inlet air receiver ("H_G gage)

(5) Exhaust receiver ("H_G gage)

(6) Static (2) and stagnation (2) in the exhaust pipe (psi from cards)

(7) Exhaust pipe mean static ("H_G gage)

(8) Cylinder pressure (psi from cards)

f. Fuel flow

DATA SHEET

Nozzle No.: 0.20 RPM: 1600

Run	T_J (°F)	T_1 (°F)	T_E (°F)	P_1 ("H_G)	Pi ("H_G)	ΔP ("H_2O)	P_{E_2} ("H_G)	P_{ATM} ("H_G)	P_{OIL} (psi)	P_{E_1} ("H_G)	Air Consumed (lb/sec)	Fuel Consumed (lb/sec)	Jet Force (lb)
3	160	71	372	13.8	12.4	22.0	0.25	29.50	50	--	0.1306	0.00200	2.71
10	150	72	500	13.6	12.1	22.0	0.25	29.50	50	--	0.1303	0.00230	3.03
13	160	73	615	13.3	11.7	22.0	0.25	29.50	50	--	0.1283	0.00270	3.43
6	163	72	480	9.8	8.8	16.0	0.15	29.50	50	--	0.1050	0.00170	2.11
11	175	72	598	9.7	8.7	16.0	0.15	29.50	50	--	0.1065	0.00210	2.53
14	166	74	744	9.4	8.2	16.0	0.20	29.50	50	--	0.1050	0.00265	2.75
9	164	72	531	7.2	6.4	12.0	0.10	29.50	50	--	0.0879	0.00200	1.79
12	175	72	682	7.0	6.2	12.0	0.10	29.50	50	--	0.0895	0.00210	2.07
15	175	74	875	5.8	6.5	12.0	0.10	29.50	50	--	0.0878	0.00275	2.57
134	150	78	377	15.4	13.8	24.0	0.20	30.10	50	1.6	0.1370	0.00160	2.68*
135	160	79	543	14.9	13.2	24.0	0.22	30.10	50	1.8	0.1368	0.00240	3.27*
136	160	80	714	14.5	12.8	24.0	0.28	30.10	50	1.8	0.1363	0.00320	3.74*
137	168	82	453	10.5	9.3	17.3	0.15	30.10	50	1.3	0.1108	0.00145	2.11*
138	170	82	580	10.4	9.3	17.0	0.18	30.10	50	1.4	0.1113	0.00205	2.47*
139	178	82	765	10.3	9.0	17.6	0.20	30.10	50	1.5	0.1130	0.00280	4.00*
140	160	82	445	7.0	6.2	11.5	0.10	30.10	50	1.2	0.0900	0.00120	1.39*
141	165	82	665	6.5	5.6	11.5	0.10	30.10	50	1.2	0.0870	0.00190	1.71*
142	170	82	800	6.5	5.2	11.8	0.10	30.10	50	1.4	0.0881	0.00235	2.03*

*Force plate readings (jet force) in error. For these runs refer to computation sheets for computed mean force ($\bar{F}$).

DATA SHEET

Nozzle No.: 0.10 RPM: 1600

Run	T_J (°F)	T_1 (°F)	T_E (°F)	P_1 ("H_G)	Pi ("H_G)	ΔP ("H_2O)	P_{E_2} ("H_G)	P_{ATM} ("H_G)	P_{OIL} (psi)	P_{E_1} ("H_G)	Air Consumed (lb/sec)	Fuel Consumed (lb/sec)	Jet Force (lb)
64	154	75	404	16.5	15.1	20.5	0.30	29.95	50	--	0.1286	0.00165	3.36
65	160	75	532	17.4	16.1	20.5	0.35	29.95	50	--	0.1320	0.00215	3.71
66	170	75	662	17.8	16.4	20.5	0.35	29.95	50	--	0.1303	0.00260	4.07
69	155	75	463	12.3	11.2	15.0	0.20	29.95	50	--	0.1058	0.00165	2.57
70	162	75	598	13.1	12.1	15.0	0.20	29.95	50	--	0.1081	0.00210	2.89
71	171	75	753	13.6	12.6	15.0	0.20	29.95	50	--	0.1072	0.00260	3.29
74	156	75	522	8.6	7.8	10.5	0.10	29.95	50	--	0.0844	0.00165	1.96
75	163	75	699	9.4	8.7	10.5	0.10	29.95	50	--	0.0859	0.00210	2.36
76	173	75	881	10.3	9.5	10.5	0.15	29.95	50	--	0.0868	0.00260	2.64
122	160	78	523	17.4	16.0	20.5	0.25	30.20	50	--	0.1310	0.00220	3.86
123	164	78	597	13.0	12.0	15.0	0.20	30.20	50	--	0.1078	0.00220	3.07
124	170	78	702	9.5	8.8	10.5	0.10	30.20	50	--	0.0860	0.00210	2.46
125	172	78	641	16.6	17.9	20.5	0.30	30.20	50	--	0.1303	0.00250	4.14
126	175	78	735	12.6	13.7	15.0	0.20	30.20	50	--	0.1072	0.00250	3.36
127	178	78	888	9.4	10.2	10.5	0.10	30.20	50	--	0.0860	0.00250	2.82

(continued)

Run	T_J (°F)	T_1 (°F)	T_E (°F)	P_1 ("H_G)	Pi ("H_G)	ΔP ("H_2O)	P_{E2} ("H_G)	P_{ATM} ("H_G)	P_{OIL} (psi)	P_{E1} ("H_G)	Air Consumed (lb/sec)	Fuel Consumed (lb/sec)	Jet Force (lb)
143	155	83	353	17.6	16.3	22.0	0.20	30.10	50	3.10	0.1360	0.00145	3.27*
144	160	82	521	19.0	17.6	22.0	0.20	30.10	50	3.50	0.1376	0.00230	3.68*
145	175	82	736	20.1	18.6	22.0	0.20	30.10	50	3.85	0.1395	0.00310	4.37*
146	175	82	756	15.1	14.2	16.5	0.15	30.10	50	3.00	0.1152	0.00280	3.26*
147	160	82	430	8.9	8.3	11.0	0.05	30.10	50	1.95	0.0875	0.00123	1.52*
148	160	82	632	9.7	8.8	11.0	0.10	30.10	50	2.05	0.0886	0.00185	1.90*
149	175	82	846	10.6	9.7	11.0	0.10	30.10	50	2.30	0.0896	0.00248	2.26*

*Force plate readings (jet force) in error. For these runs refer to computation sheets for computed mean force ($\bar{F}$).

DATA SHEET

Nozzle No.: 0.05 RPM: 1600

Run	T_J (°F)	T_1 (°F)	T_E (°F)	P_1 ("H_G)	Pi ("H_G)	ΔP ("H_2O)	P_{E2} ("H_G)	P_{ATM} ("H_G)	P_{OIL} (psi)	P_{E1} ("H_G)	Air Consumed (lb/sec)	Fuel Consumed (lb/sec)	Jet Force (lb)
79	155	81	437	21.5	20.2	19.0	0.30	29.90	50	--	0.1310	0.00175	3.86
80	168	81	563	24.0	22.6	20.0	0.35	29.90	50	--	0.1388	0.00205	4.22
81	171	81	705	24.7	23.4	19.0	0.30	29.90	50	--	0.1343	0.00250	4.50
84	158	81	479	17.6	16.6	15.0	0.20	29.90	50	--	0.1125	0.00162	3.00
85	168	82	628	19.4	18.4	15.0	0.20	29.90	50	--	0.1159	0.00210	3.46
86	173	81	773	20.8	19.8	15.0	0.15	29.90	50	--	0.1168	0.00250	3.86
89	160	82	546	13.0	12.3	10.0	0.10	29.90	50	--	0.0870	0.00162	2.29
90	168	82	731	14.6	13.9	10.0	0.10	29.90	50	--	0.0894	0.00210	2.72
91	178	81	926	16.0	15.3	10.0	0.10	29.90	50	--	0.0863	0.00255	3.07
128	180	81	760	37.0	34.8	30.0	0.50	30.15	50	11.0	0.1900	0.00370	7.11
129	160	81	725	28.3	26.4	22.0	0.30	30.15	50	8.0	0.1500	0.00300	5.35
130	180	81	846	29.0	27.3	22.0	0.20	30.15	50	8.5	0.1520	0.00365	5.78
131	180	81	637	20.1	17.2	16.0	0.15	30.15	50	5.5	0.1195	0.00220	3.64
132	180	84	850	22.3	21.3	16.0	0.15	30.15	50	6.4	0.1227	0.00295	4.28
133	180	84	1014	23.9	22.7	16.0	0.20	30.15	50	7.1	0.1245	0.00360	4.86

DATA SHEET

Nozzle No.: 0.025 RPM: 1600

Run	T_J (°F)	T_1 (°F)	T_E (°F)	P_1 ("H_G)	Pi ("H_G)	ΔP ("H_2O)	P_{E_2} ("H_G)	P_{ATM} ("H_G)	P_{OIL} (psi)	P_{E_1} ("H_G)	Air Consumed (lb/sec)	Fuel Consumed (lb/sec)	Jet Force (lb)
18	160	81	475	27.6	26.5	18.0	0.10	29.80	50	--	0.1350	0.00180	4.40
25	175	80	624	31.6	30.3	18.0	0.15	29.80	50	--	0.1414	0.00225	4.96
28	168	83	735	35.4	34.0	18.0	0.25	29.80	50	--	0.1430	0.00275	5.74
21	160	80	521	22.4	21.5	14.0	0.10	29.80	50	--	0.1140	0.00175	3.43
26	170	75	671	25.5	24.4	14.0	0.10	29.80	50	--	0.1192	0.00220	4.03
29	170	83	829	28.5	27.6	14.0	0.15	29.80	50	--	0.1200	0.00275	4.50
24	160	80	588	17.4	16.6	10.0	0.10	29.80	50	--	0.0912	0.00175	2.50
27	170	81	740	20.1	19.2	10.0	0.10	29.80	50	--	0.0945	0.00215	3.15
30	175	83	956	22.5	21.8	10.0	0.10	29.80	50	--	0.0964	0.00275	3.44
150	160	79	471	21.4	20.5	13.0	0.10	30.10	50	9.85	0.1094	0.00150	2.95*
151	175	79	744	26.0	25.1	13.0	0.10	30.10	49	12.50	0.1152	0.00225	3.35*
152	185	79	1061	32.3	31.5	13.5	0.10	30.10	50	16.90	0.1200	0.00330	5.15*

*Force plate readings (jet force) in error. For these runs refer to computation sheets for computed mean force ($\bar{F}$).

SAMPLE EXHAUST PIPE PRESSURE CARDS

NOZZLE NO	R_s	F/A
0.025	0.90	0.0370
0.05	1.19	0.0371
0.10	0.98	0.0388
0.20	1.00	0.0375

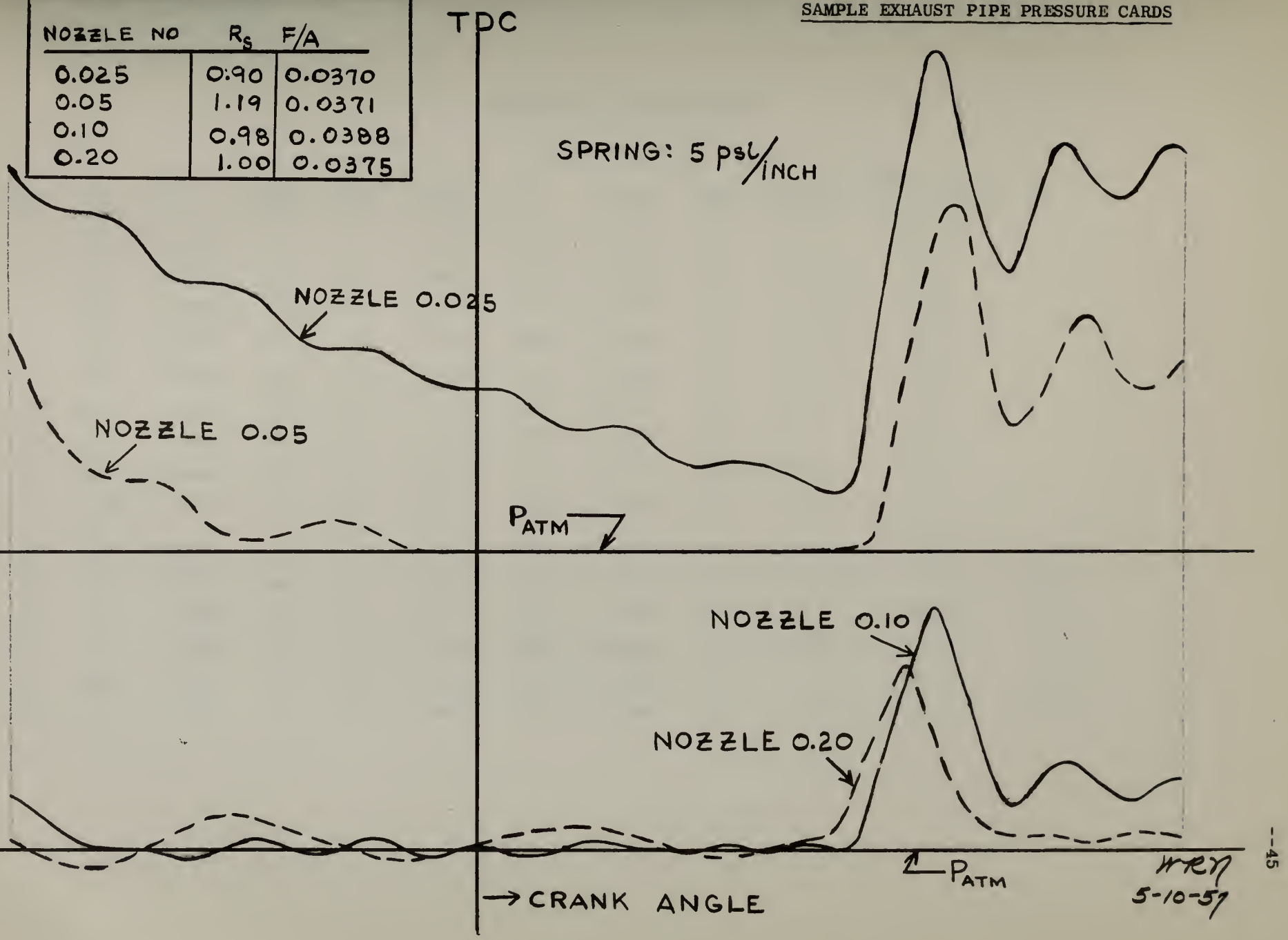

HRM
5-10-57

SUMMARY OF COMPUTATIONS

Nozzle No.: 0.20

Run	R_S	F/A	$BMEP_M$	FMEP	$IMEP_E$	P_R	M_A+M_F	$TMEP_R$	$CMEP_R$	$(IMEP)_{R_{Total}}$	$\bar{F}$
3	1.45	0.0267	13.1	55	68.1	1.420	0.1300	5.8	8.4	65.5	
6	1.18	0.0248	13.1	55	68.1	1.298	0.1067	4.1	5.1	67.1	
9	0.99	0.0323	13.1	55	68.1	1.218	0.0899	3.6	3.2	68.5	
10	1.48	0.0310	34.6	55	89.6	1.228	0.1303	6.8	5.0	91.4	
11	1.19	0.0306	34.6	55	89.6	1.127	0.1086	5.9	2.3	93.2	
12	1.03	0.0336	34.6	55	89.6	1.052	0.0915	4.6	0.8	93.4	
13	1.41	0.0362	58.5	55	113.5	1.396	0.1310	9.1	8.3	114.3	
14	1.17	0.0389	58.5	55	113.5	1.278	0.1077	7.1	4.8	115.8	
15	0.99	0.0443	58.5	55	113.5	1.230	0.0906	7.2	3.2	117.5	
134	1.53	0.0210	11.2	55	66.2	1.512	0.1386	1.6	10.9	56.9	1.49
135	1.52	0.0314	48.6	55	103.6	1.440	0.1392	5.5	10.2	98.9	2.79
136	1.52	0.0420	82.7	55	137.7	1.428	0.1395	5.7	9.3	134.1	2.84
140	1.02	0.0190	3.9	55	58.9	1.208	0.0912	2.1	3.0	58.0	1.37
141	0.99	0.0309	26.8	55	81.8	1.188	0.0889	8.6	2.7	87.7	2.77
142	1.00	0.0375	45.3	55	100.3	1.172	0.0855	8.7	2.5	106.7	2.76

SUMMARY OF COMPUTATIONS

Nozzle No.: 0.10

Run	R_S	F/A	$BMEP_M$	FMEP	$IMEP_E$	P_R	M_A+M_F	$TMEP_R$	$CMEP_R$	$(IMEP)_{R_{Total}}$	$\bar{F}$
64	1.35	0.0213	13.1	55	68.1	1.505	0.1303	8.7	10.1	66.7	
69	1.16	0.0238	13.1	55	68.1	1.375	0.1075	6.3	6.5	67.9	
74	0.92	0.0266	13.1	55	68.1	1.261	0.0861	4.4	3.6	68.9	
65	1.32	0.0265	35.8	55	90.8	1.520	0.1341	10.5	10.6	90.7	
70	1.15	0.0295	35.8	55	90.8	1.394	0.1102	7.9	6.8	91.9	
75	0.92	0.0333	35.8	55	90.8	1.348	0.0880	6.2	4.9	92.1	
66	1.35	0.0333	58.5	55	113.5	1.550	0.1329	12.5	11.1	114.9	
71	1.13	0.0365	58.5	55	113.5	1.420	0.1098	10.0	7.2	116.3	
76	0.93	0.0410	58.5	55	113.5	1.320	0.0894	7.9	4.6	116.8	
122	1.32	0.0277	34.6	55	89.6	1.533	0.1332	11.0	10.7	89.9	
123	1.11	0.0307	34.6	55	89.6	1.400	0.1100	8.5	6.9	91.2	
124	0.87	0.0317	34.6	55	89.6	1.295	0.0881	6.7	4.2	92.1	
125	1.27	0.0309	57.2	55	112.2	1.595	0.1328	12.8	11.9	113.1	
126	1.11	0.0350	57.2	55	112.2	1.460	0.1097	10.2	7.8	114.6	
127	0.92	0.0399	57.2	55	112.2	1.342	0.0885	9.0	4.8	116.4	

(Continued)

Run	R_S	F/A	$BMEP_M$	FMEP	$IMEP_E$	P_R	M_A+M_F	$TMEP_R$	$CMEP_R$	$(IMEP)_{R_{Total}}$	$\bar{F}$
143	1.46	0.0187	1.1	55	56.1	1.541	0.1375	11.2	11.4	55.9	3.95
144	1.46	0.0292	40.2	55	95.2	1.585	0.1401	12.2	12.4	95.0	4.17
145	1.46	0.0388	81.0	55	136.0	1.620	0.1426	12.4	13.6	134.8	4.23
146	1.23	0.0383	64.8	55	119.8	1.475	0.1180	11.8	8.6	123.0	3.75
147	0.98	0.0197	3.4	55	58.4	1.278	0.0887	4.7	4.0	59.1	2.03
148	0.98	0.0292	26.2	55	81.2	1.294	0.0901	6.6	4.3	83.5	2.46
149	0.98	0.0388	50.8	55	105.8	1.323	0.0921	7.4	4.8	108.4	2.62

SUMMARY OF COMPUTATIONS

Nozzle No.: 0.05

Run	R_S	F/A	$BMEP_M$	FMEP	$IMEP_E$	P_R	M_A+M_F	$TMEP_R$	$CMEP_R$	$(IMEP)_{R_{Total}}$	$\bar{F}$
79	1.30	0.0217	13.1	55	68.1	1.675	0.1328	11.3	13.2	66.2	
84	1.15	0.0218	13.1	55	68.1	1.558	0.1141	8.0	9.6	66.5	
89	0.92	0.0253	13.1	55	68.1	1.412	0.0986	5.5	5.7	67.9	
80	1.35	0.0246	35.8	55	90.8	1.802	0.1402	12.8	15.3	88.3	
85	1.17	0.0281	35.8	55	90.8	1.616	0.1180	10.3	10.6	90.5	
90	0.94	0.0323	35.8	55	90.8	1.465	0.0915	8.2	6.5	92.5	
81	1.30	0.0301	58.5	55	113.5	1.782	0.1368	14.9	15.6	112.8	
86	1.16	0.0329	58.5	55	113.5	1.661	0.1183	12.8	11.8	114.5	
91	0.89	0.0386	58.5	55	113.5	1.510	0.0889	10.6	6.9	117.2	
128	1.62	0.0361	101.6	55	156.6	2.155	0.1937	26.2	29.8	153.0	
129	1.38	0.0337	73.8	55	128.8	1.880	0.1530	18.7	19.5	128.0	
130	1.38	0.0403	89.3	55	144.3	1.905	0.1559	21.4	19.6	146.1	
132	1.19	0.0371	72.0	55	127.2	1.705	0.1257	14.4	12.9	128.7	
133	1.18	0.0443	95.0	55	150.0	1.755	0.1281	17.4	13.9	153.5	

SUMMARY OF COMPUTATIONS

Nozzle No.: 0.025

Run	R_S	F/A	$BMEP_M$	FMEP	$IMEP_E$	P_R	M_A+M_F	$TMEP_R$	$CMEP_R$	$(IMEP)_{R\,Total}$	$\bar{F}$
18	1.08	0.0197	13.1	55	68.1	1.890	0.1368	14.2	17.3	65.0	
21	0.98	0.0215	13.1	55	68.1	1.720	0.1165	10.2	12.7	65.6	
24	0.85	0.0250	13.1	55	68.1	1.560	0.1090	5.9	8.0	66.0	
25	0.97	0.0220	34.6	55	89.6	2.005	0.1416	17.2	20.0	86.8	
26	0.98	0.0257	34.6	55	89.6	1.815	0.1194	13.2	14.2	88.6	
27	0.81	0.0293	34.6	55	89.6	1.638	0.0966	10.1	9.2	90.5	
28	1.04	0.0278	58.5	55	113.5	2.140	0.1458	22.9	22.2	114.2	
29	0.96	0.0318	58.5	55	113.5	1.930	0.1228	16.6	16.0	114.1	
30	0.85	0.0377	58.5	55	113.5	1.731	0.0991	11.2	10.5	114.2	
150	0.98	0.0193	5.6	55	60.6	1.683	0.1109	9.8	11.1	59.3	3.31
151	0.96	0.0270	40.2	55	95.2	1.832	0.1174	12.8	13.9	94.1	3.90
152	0.90	0.0370	80.4	55	130.4	2.05	0.1233	21.4	16.9	134.9	5.16

Figure XVI

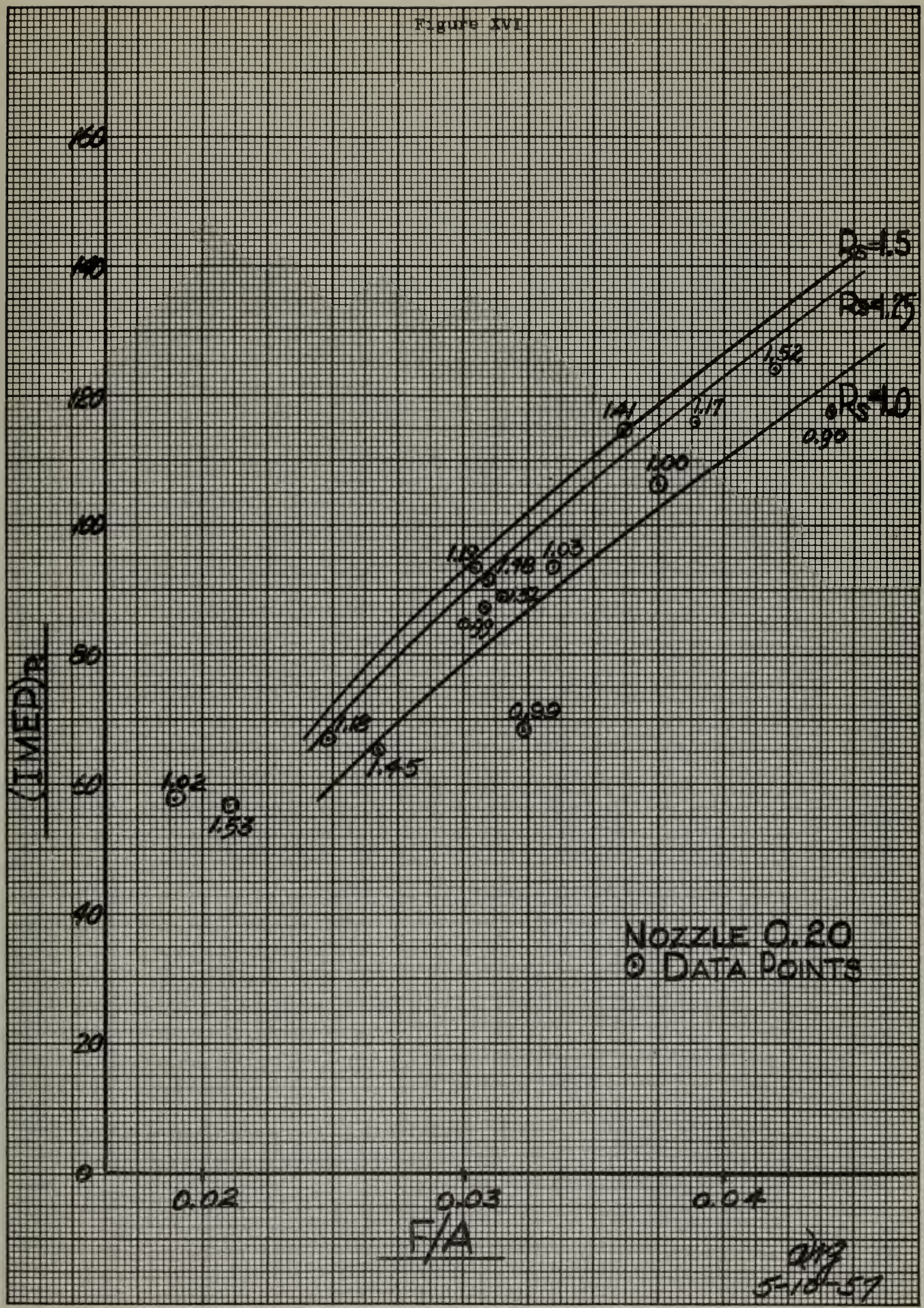

160
140
120
100
80
60
40
20
0
(IMEP)R
0.02
0.03
0.04
F/A
Rs=1.5
Rs=1.25
Rs=1.0
1.52
1.41
1.17
0.90
1.00
1.19
1.48
1.03
1.52
0.99
1.18
0.99
1.45
1.02
1.53
NOZZLE 0.20
⊙ DATA POINTS
5-10-57

Figure XVIII

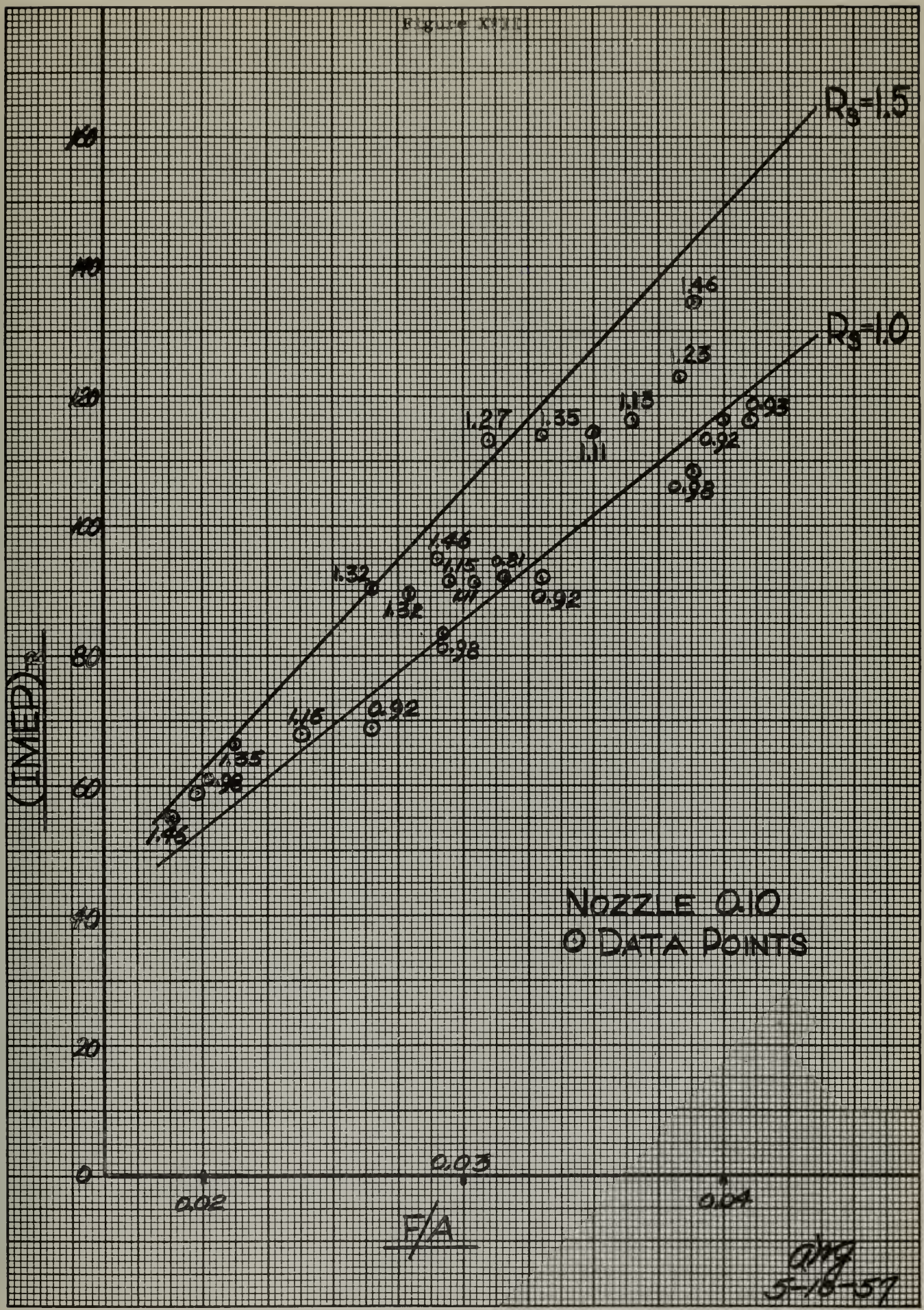

Figure XV-11

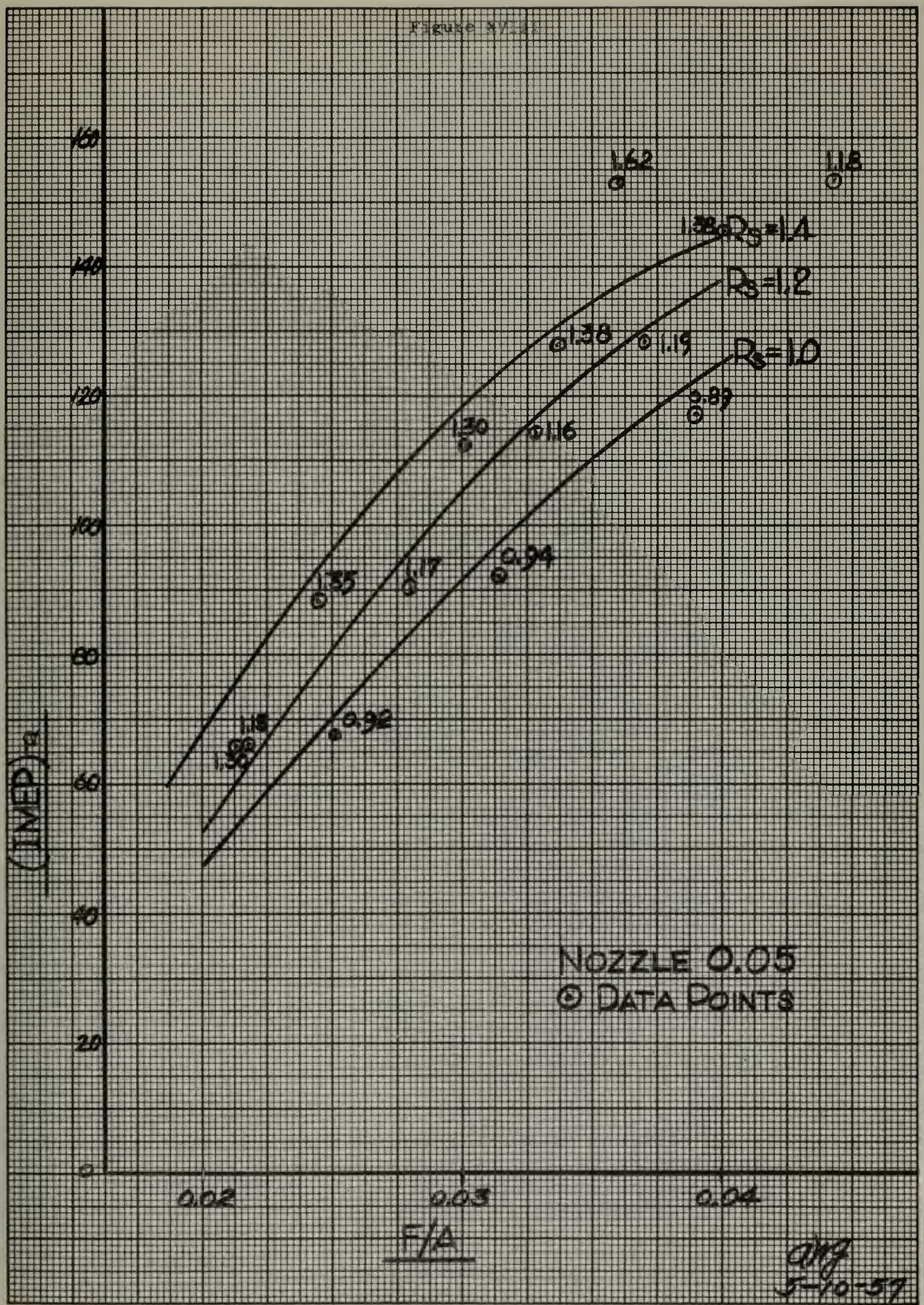
160
140
120
100
80
60
40
20
0
(IMEP)gr
0.02
0.03
0.04
F/A
1.62
1.8
1.38
R_S=1.4
R_S=1.2
R_S=1.0
1.38
1.19
1.30
1.16
1.35
1.17
0.94
1.18
1.36
0.92
0.89
NOZZLE 0.05
⊙ DATA POINTS
5-10-57

Figure XIX

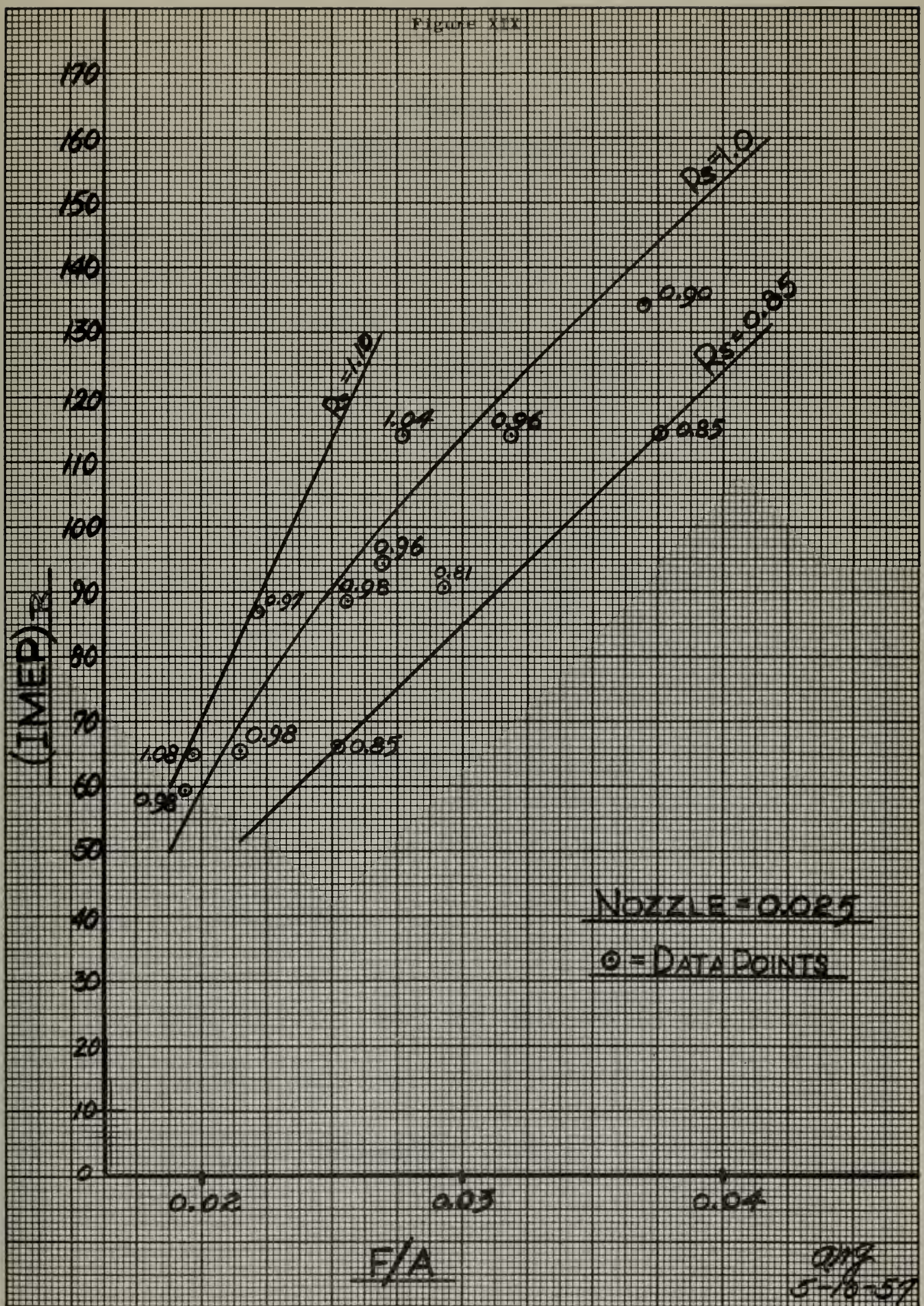
(IMEP) psi
170
160
150
140
130
120
110
100
90
80
70
60
50
40
30
20
10
0
0.02
0.03
0.04
F/A
Rs=1.0
Rs=0.85
1.04
0.96
0.90
0.85
0.96
0.98
0.81
0.97
1.08
0.98
0.98
0.85
NOZZLE = 0.025
⊙ = DATA POINTS
DNF
5-10-57

APPENDIX D

SUMMARY OF CALCULATIONS

Example: Run 86

Nozzle No.: 0.05

1. Calculation of scavenging ratio (R_S)

   a. From P_1, Pi, and ΔP and using Leary and Tsai's orifice analysis

$$Ma = (\text{air flow}) \sqrt{\frac{(Pi + P_{ATM})}{30.00} \times \frac{540}{T_1}} \; (Y)$$

   for air flow see Figure XX

   for expansion factor Y see Figure XXI

$$Ma = (0.0915) \sqrt{\frac{(19.80 + 29.90)}{30.00} \times \frac{540}{541}} \; (0.987)$$

$$Ma = 0.1168$$

   b. $$R_S = \frac{60\ Ma}{\rho_S\ N\ V_C}$$

$$\rho_S = \frac{P_{E1}}{R\ T_1} = \frac{(35.2)(0.491)(144)}{(53.3)(541)} = 0.0862 \text{ lb/ft}^3$$

$$N = 1600 \text{ rpm}$$

$$V_C = 0.0435 \text{ ft}^3$$

$$R_S = \frac{(60)(0.1168)}{(0.0862)(1600)(0.0435)} = 1.165$$

2. Calculation of fuel-air ratio (F/A)

   a. Knowing $R_S = 1.165$, enter Figure XXII, and pick off $\eta_S = 0.76$

   b. $$\Gamma = \frac{\eta_S}{R_S} = \frac{0.76}{1.165} = 0.652$$

   c. $$\frac{F}{A} = \frac{\Gamma\ M_A}{M_F} = \frac{(0.652)(0.1168)}{(0.00250)} = 0.0329$$

Figure XX

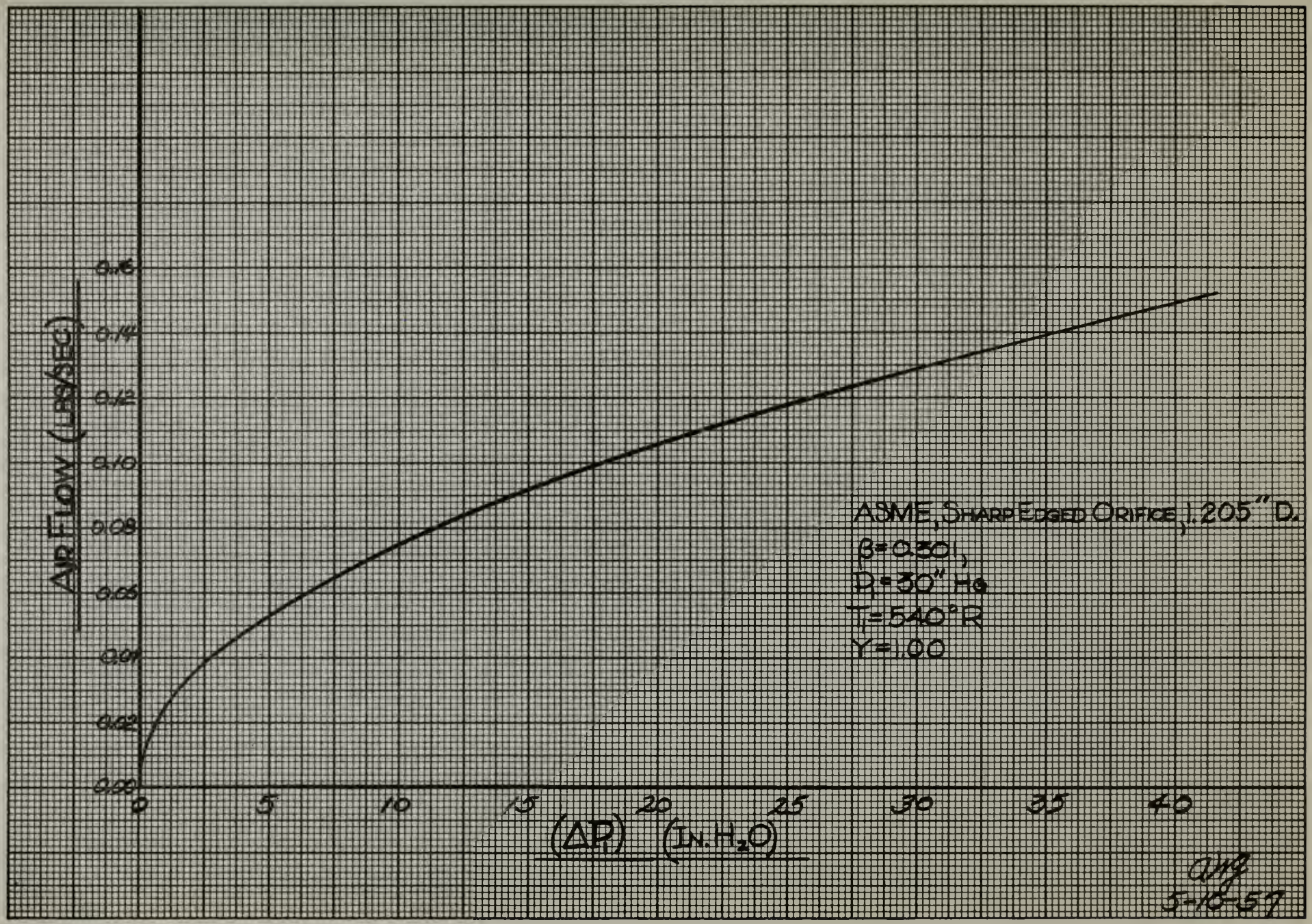
AIR FLOW (LBS/SEC)
0.16
0.14
0.12
0.10
0.08
0.06
0.04
0.02
0.00
0
5
10
15
20
25
30
35
40
(ΔP1) (IN. H2O)
ASME, SHARP EDGED ORIFICE, 1.205" D.
β=0.301,
P1=30" HG
T1=540°R
Y=1.00
5-10-57

Figure XXI

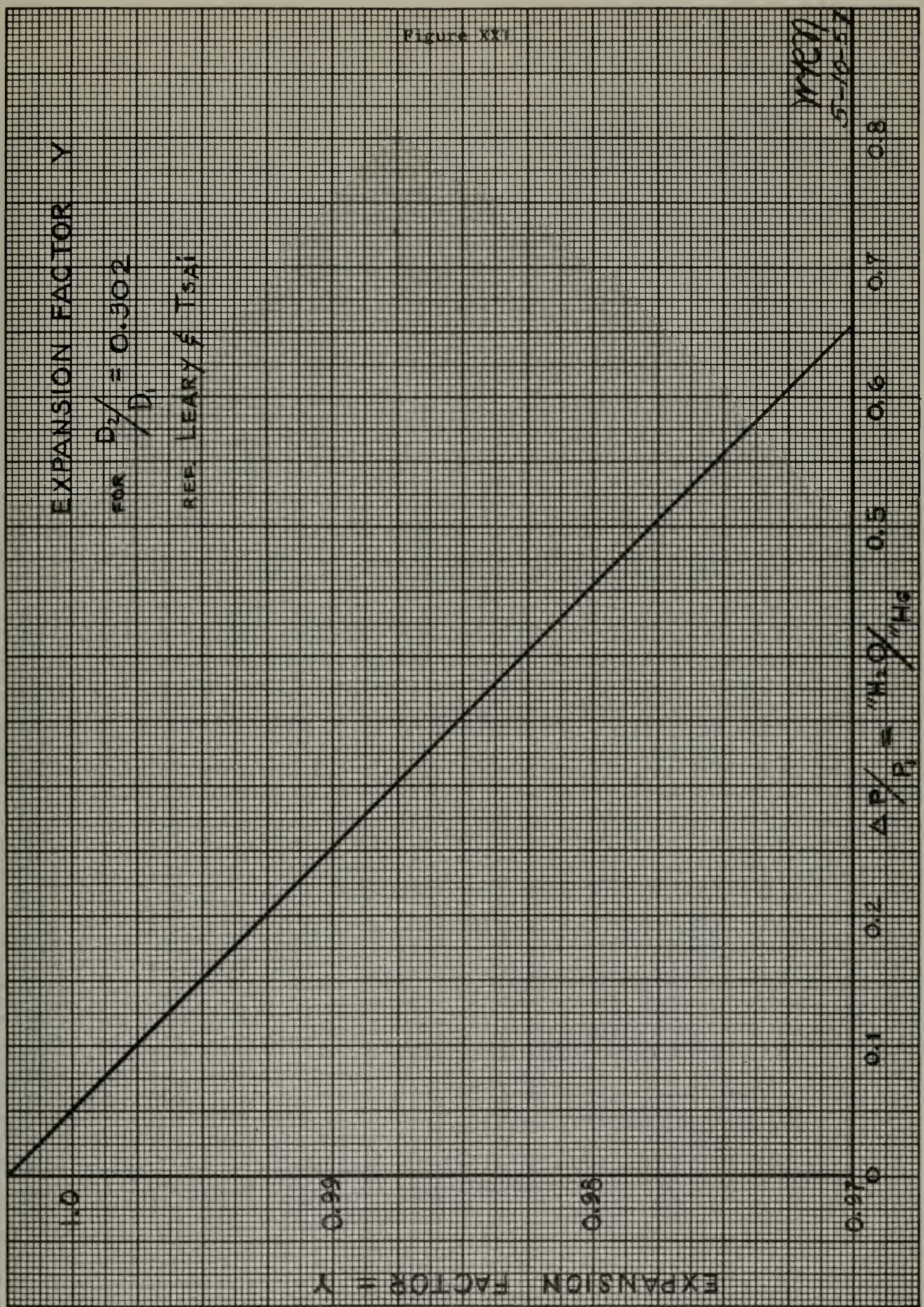
EXPANSION FACTOR Y
FOR $D_2/D_1 = 0.902$
REF. LEARY & TSAI
EXPANSION FACTOR = Y
1.0
0.99
0.98
0.97
0
0.1
0.2
0.3
0.4
0.5
0.6
0.7
0.8
0.9
$\Delta P/P_1 = mH_2O/mH_2O$

Figure XXII

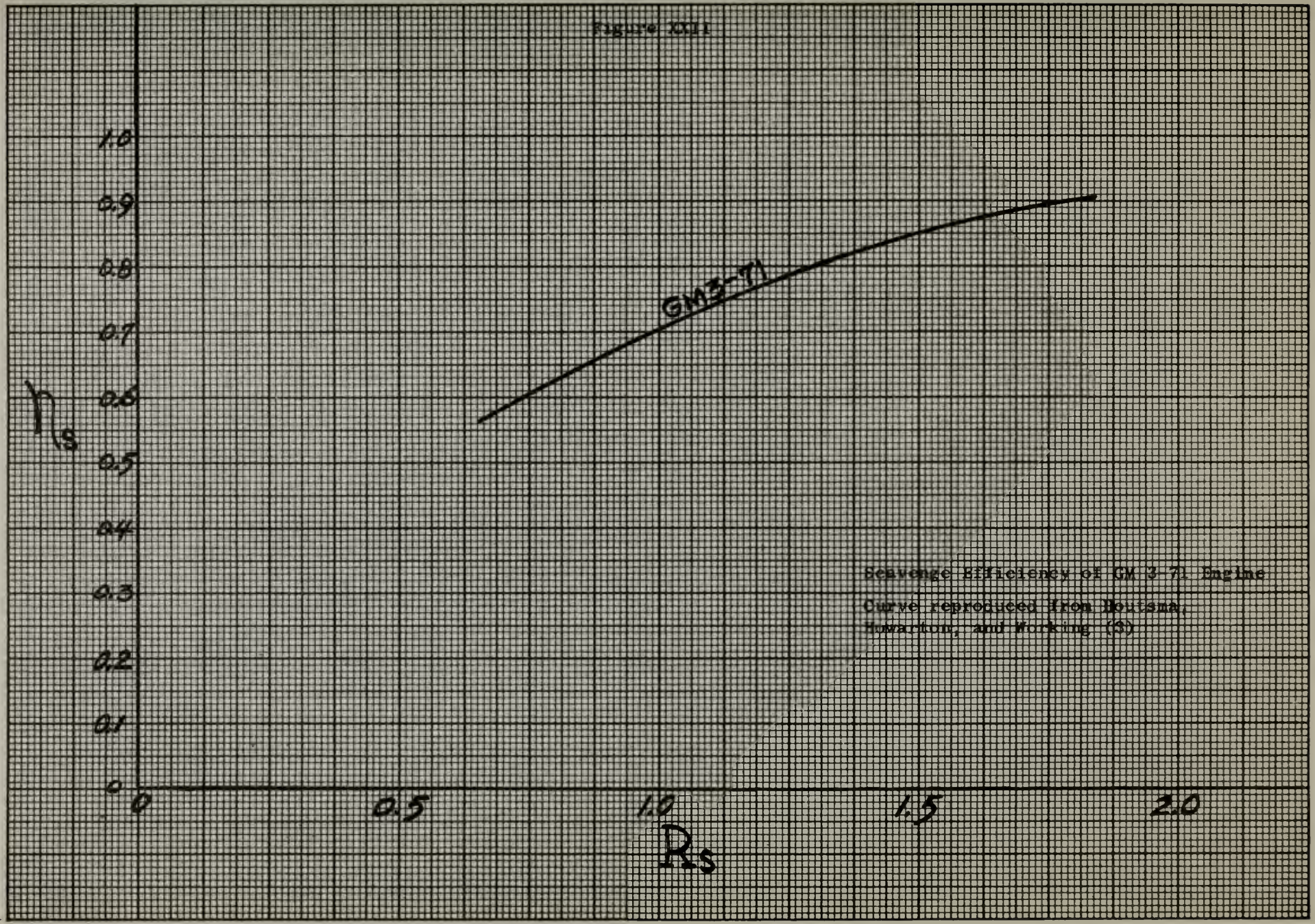

Scavenge Efficiency of GM 3-71 Engine

Curve reproduced from Boutsma, Howarth, and Working (3)

3. Calculation of $TMEP_R$

a. From Appendix A

$$\text{Power} = \frac{F^2}{2(M_A + M_F)}$$

$$THP_R = \frac{F^2}{2(M_A + M_F)} \times \frac{32.2}{550}$$

See Figure XXIII for plot of $(THP)_R (M_A + M_F)$ vs. F

$M_A + M_F = 0.1168 + 0.00250 = 0.1193$

$F = 3.86$ lb

From Figure XXIII, $(M_A + M_F)(THP)_R = 0.430$

$$THP_R = \frac{0.430}{0.1193} = 3.60 \text{ h.p.}$$

b. $$(THP)_R = \frac{(TMEP)_R \; L \; A \; N}{(33{,}000)(12)}$$

L = stroke = 5 in.

A = piston area = 14.1 in.^2

N = 1600 rpm

$$TMEP_R = \frac{(3.60)(33{,}000)(12)}{(5)(14.1)(1600)}$$

$TMEP_R = 12.8$ psi

4. Calculation of $CMEP_R$

a. $\text{Compressor work}_{\text{Isentropic}} = W_c = C_p (T_2 - T_1) = C_p T_1 (\frac{T_2}{T_1} - 1)$

where state 1 = atmospheric pressure

state 2 = supercharge level (inlet pressure)

b. $W_c = C_p T_1 (P_R^{\frac{K-1}{K}} - 1)$ $\quad P_R = \frac{Pi + P_{ATM}}{P_{ATM}}$

c. $\text{Power} = \frac{M_A J C_p T_1}{550} (P_R^{\frac{K-1}{K}} - 1)$ $\quad J = 778 \frac{\text{ft-lbs}}{\text{Btu}}$

d. $CHP_R = \frac{M_A J C_p T_1}{550} (P_R^{\frac{K-1}{K}} - 1)$

Figure XXIII

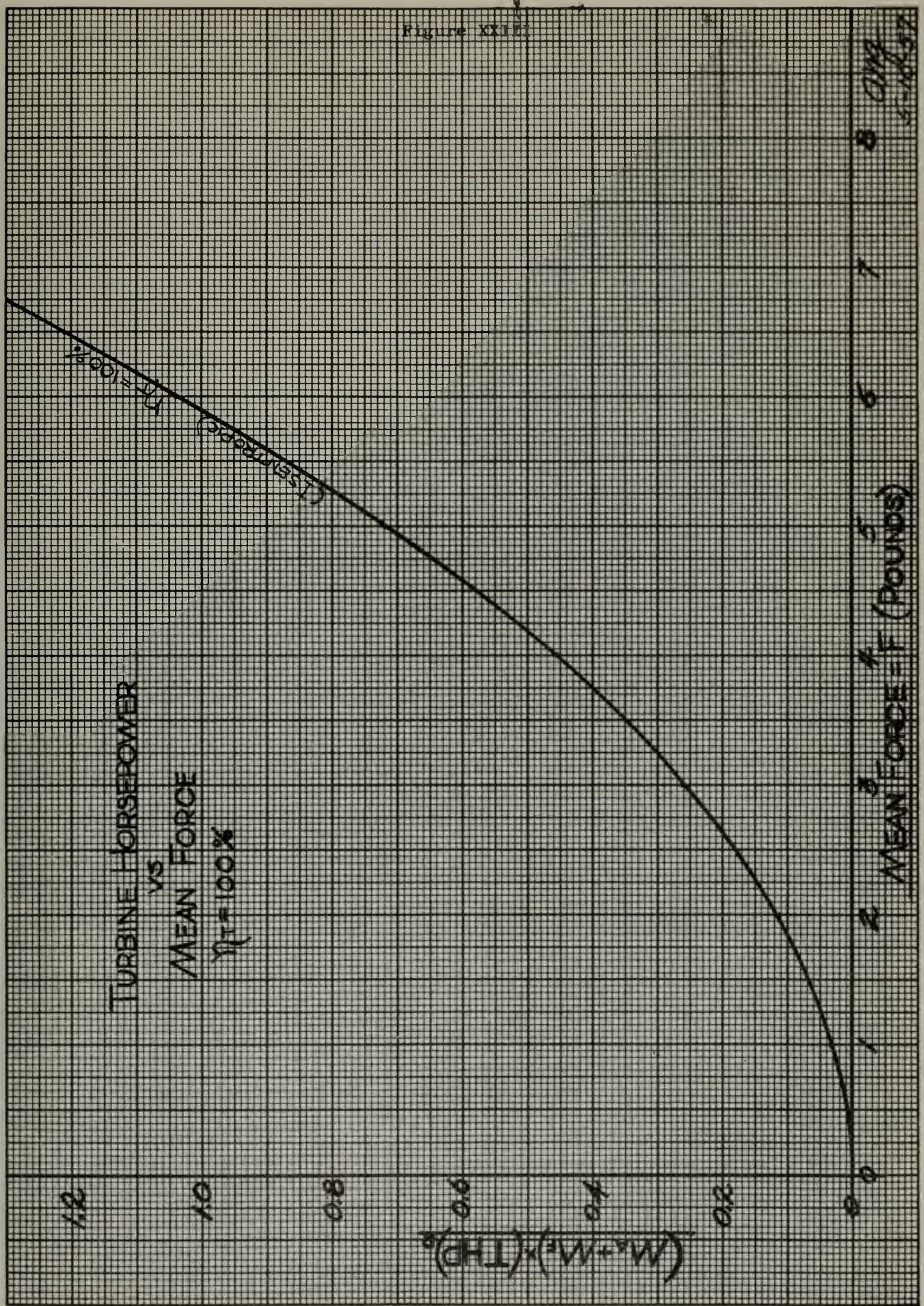

Figure XXIV

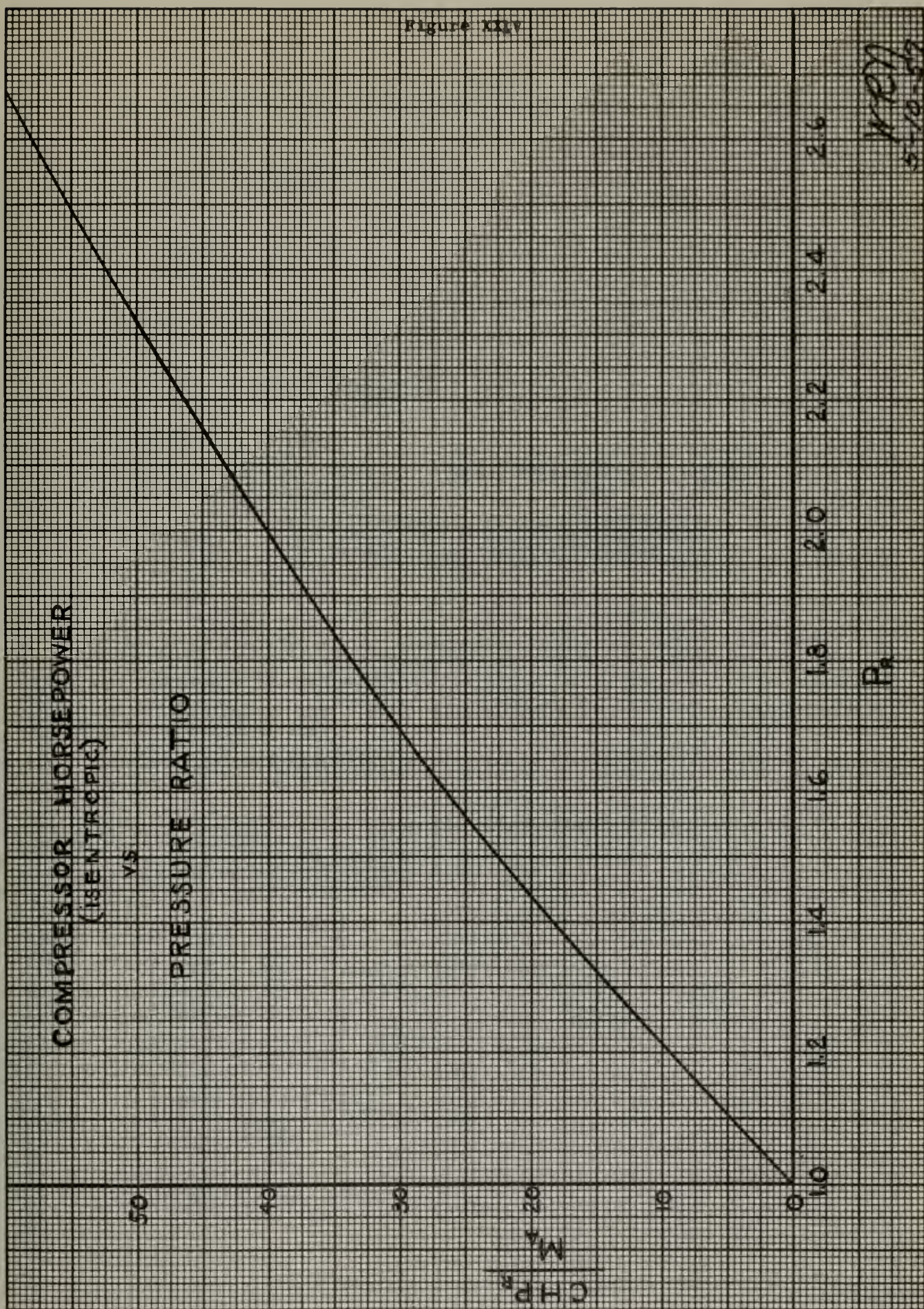
COMPRESSOR HORSEPOWER
(ISENTROPIC)
VS
PRESSURE RATIO
$\frac{CHP_R}{M_A}$
0
10
20
30
40
50
1.0
1.2
1.4
1.6
1.8
2.0
2.2
2.4
2.6
P_R
WRJ
5-10-57

e. See Figure XXIV, for plot of $\frac{CHP_R}{M_A}$ vs. P_R

f. $P_R = \frac{19.80 + 29.90}{29.90} = 1.66$

$\frac{CHP_R}{M_A} = 28.8$

g. $M_A = 0.1168 \qquad CHP_R = 28.8\ (0.1168) = 3.36$ h.p.

$CMEP_R = \frac{(3.36)(33,000)(12)}{(5)(14.1)(1600)} = 11.8$ psi

5. Calculation of $BMEP_M$

a. $BHP_M = \frac{\text{brake load } (''H_G) \text{ x rpm}}{\text{dynamometer constant}} = \frac{(B.L.)(1600)}{1000} = 1.6$ B.L.

b. $BMEP_M = \frac{(BHP_M)(33,000)(12)}{L\ A\ N} = \frac{(1.6\ B.L.)(33,000)(12)}{(5)(14.1)(1600)}$

$BMEP_M = 5.58$ B.L.

c. B.L. = 10.25 $''H_G$

$BMEP_M = (5.58)(10.25) = 57.2$ psi

6. Calculation of FMEP

a. $FMEP = \frac{FHP\ (33,000)(12)}{L\ A\ N}$

b. FHP = 16 (average value used from motoring runs)

$FMEP = \frac{(16)(33,000)(12)}{(5)(14.1)(1600)} = 56.3$ psi

7. Calculation of $IMEP_R$

a. $IMEP_R = BMEP_M + FMEP + TMEP_R - CMEP_R$

$IMEP_R = 57.2 + 56.3 + 12.8 - 11.8 = 114.5$ psi

8. Calculation of $BMEP_T$ $(\eta_C = \eta_T = 0.75)$

a. $TMEP = 0.75\ (TMEP_R)$

$CMEP = \frac{CMEP_R}{.75}$

$IMEP_E = BMEP_M + FMEP$

b. $BMEP_T = IMEP_E - 1/3\ FMEP + TMEP - CMEP$

$$BMEP_T = 57.2 + 56.3 - 1/3\ (56.3) + (0.75)(12.8) - \frac{(11.8)}{0.75}$$

$$BMEP_T = 88.6 \text{ psi}$$

9. Calculation of $\frac{TMEP - CMEP}{BMEP_T}$

$$\frac{TMEP - CMEP}{BMEP_T} = \frac{9.6 - 15.7}{88.6} = -0.0688 = -6.8\%$$

Note: $\frac{TMEP-CMEP}{BMEP_T}$ plot was calculated and drawn from cross plots of

TMEP, CMEP, and $BMEP_T$

10. Calculation of BSFC

a. $$BSFC = \frac{(\Gamma)(M_A)(F/A)}{BHP_T}$$

b. $$BHP_T = \frac{(BMEP_T)(5)(14.1)(1600)}{(33,000)(12)}$$

c. $$BSFC = \frac{(0.652)(0.1168)(0.0329)(33,000)(12)}{(88.6)(5)(14.1)(1600)}$$

$$BSFC = 0.356\ \frac{\text{lbs}}{BHP_T\text{-hr}}$$

Note: BSFC curve was calculated and drawn from cross plots

Figure XXV

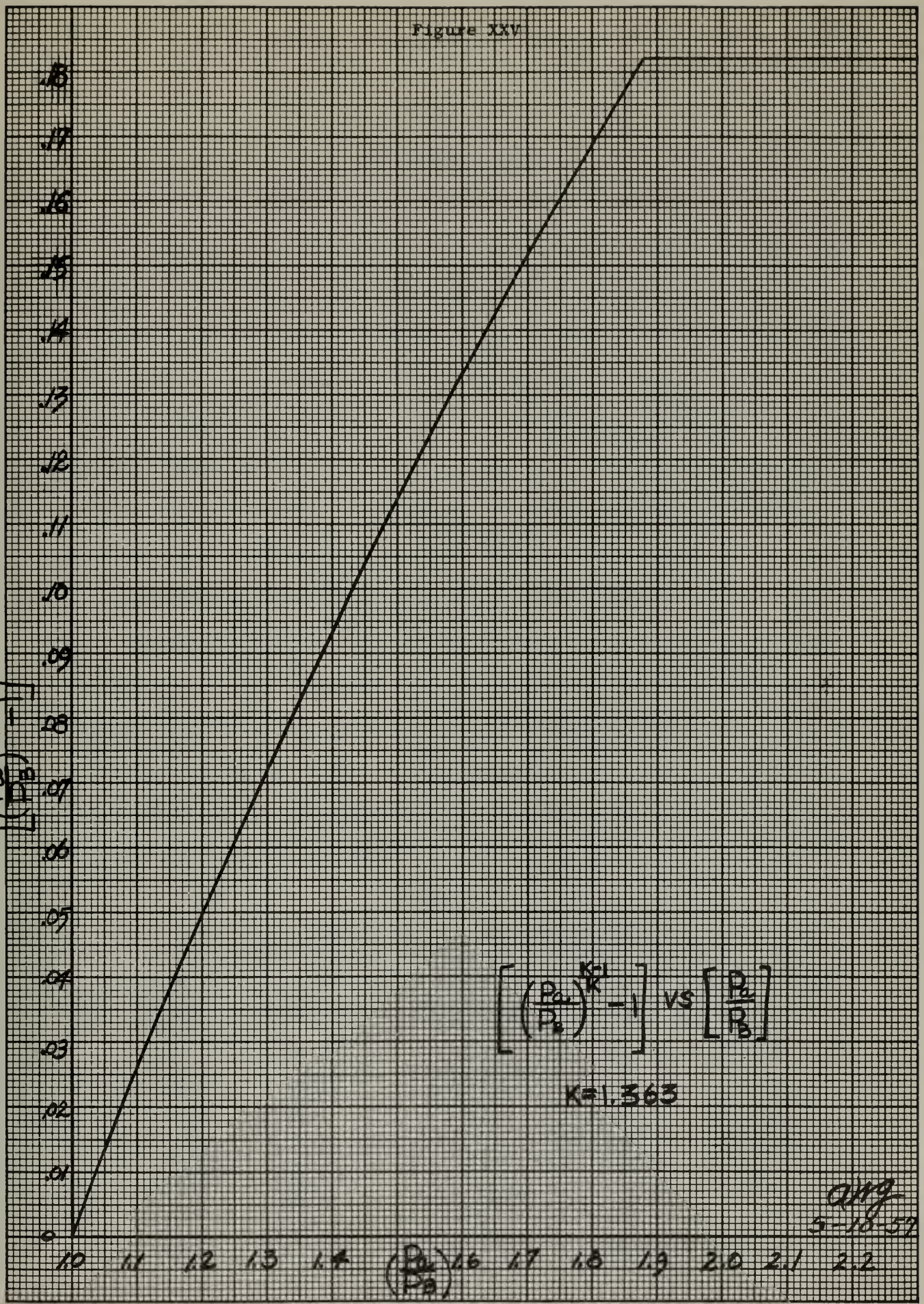
.16
.15
.14
.13
.12
.11
.10
.09
.08
.07
.06
.05
.04
.03
.02
.01
0
1.0
1.1
1.2
1.3
1.4
1.6
1.7
1.8
1.9
2.0
2.1
2.2
$\left[\left(\frac{P_a}{P_B}\right)^{\frac{K-1}{K}}-1\right]$
$\left[\frac{P_a}{P_B}\right]$
$\left[\left(\frac{P_a}{P_B}\right)^{\frac{K-1}{K}}-1\right]$ vs $\left[\frac{P_a}{P_B}\right]$
K=1.363
WJG
5-16-52

APPENDIX E

ENGINE FRICTION

A predicted FMEP was used for all calculations covered in this investigation. The FMEP was predicted on the basis of friction horsepower measured while motoring at several values of rpm and inlet air pressure. Figure XXVI is the result of these motoring friction measurements. A value of FMEP of 55 psi was chosen for calculation purposes as a representative mean for the runs made at 1600 rpm. A check on the validity of this choice was made by planimetering engine indicator P-V diagrams for IMEP, and subtracting the measured BMEP to obtain FMEP.

Table III presents the results of a number of checks made on runs representative of a wide range of operating conditions. While for the majority of the check points the results can be considered within experimental error, it is apparent that the taking of engine indicator cards for every run, to determine the IMEP and thus the actual FMEP is the obvious way to eliminate any error introduced into the calculations by using only a predicted FMEP.

TABLE III

COMPARISON OF MOTORING AND INDICATOR CARD FRICTION

Run No.	IMEP (Card)	IMEP (Predicted)	BMEP (Measured)	FMEP (Actual)	$\frac{(FMEP-55)}{55} \times 100$
10	107.0	89.6	34.6	72.4	+31.6%
25	106.2	89.6	34.6	72.2	+31.3%
122	96.7	89.6	34.6	62.1	+12.9%
142	98.8	100.3	45.3	53.5	- 2.7%
149	109.7	105.8	50.8	58.9	+ 7.1%
150	65.8	60.6	5.6	60.2	+ 9.5%
151	108.2	95.2	40.2	68.0	+23.6%

Figure XXVI

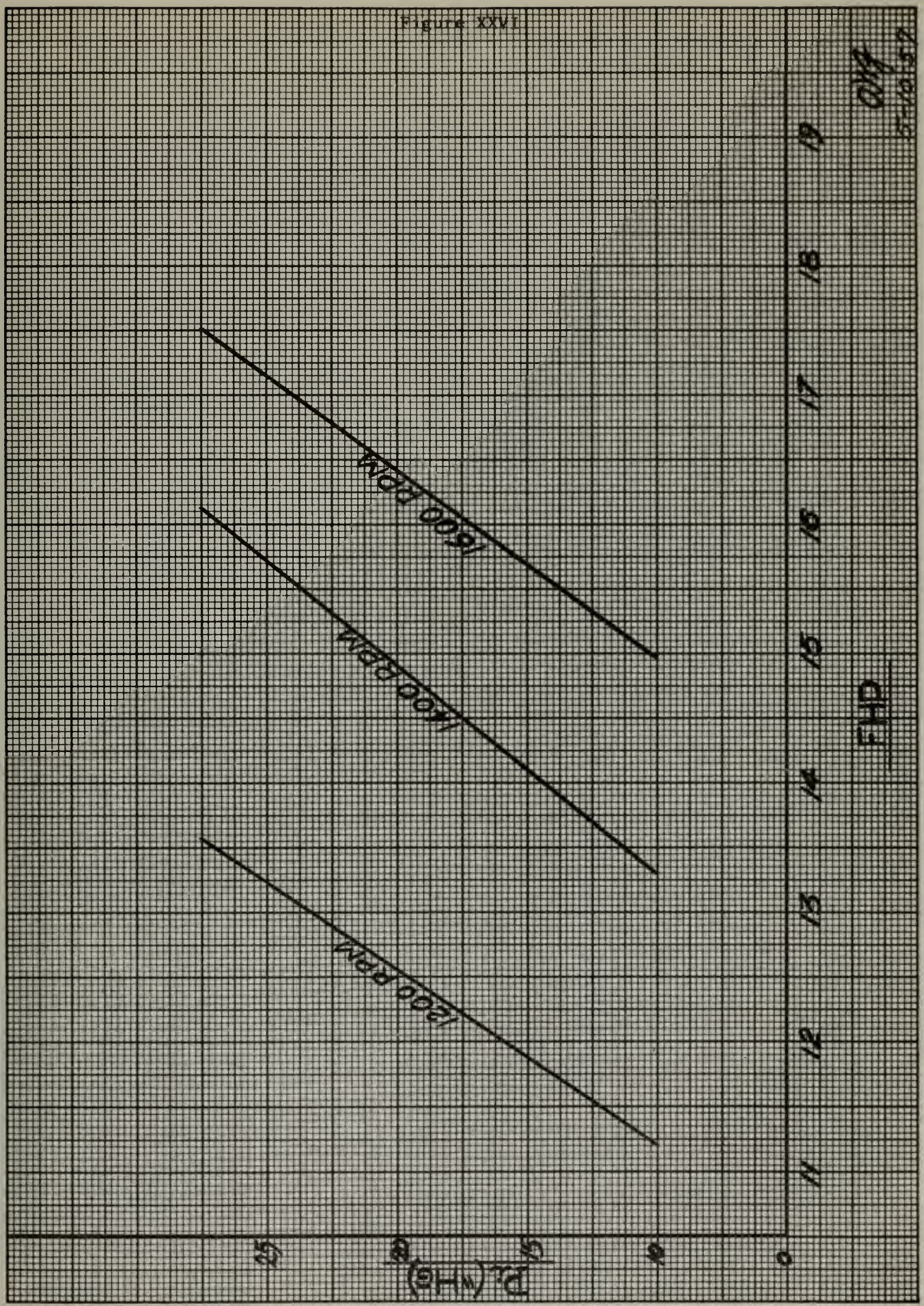
1600 RPM
1400 RPM
1200 RPM
FHP
11
12
13
14
15
16
17
18
19
0
10
15
20
25

Figure XXVII

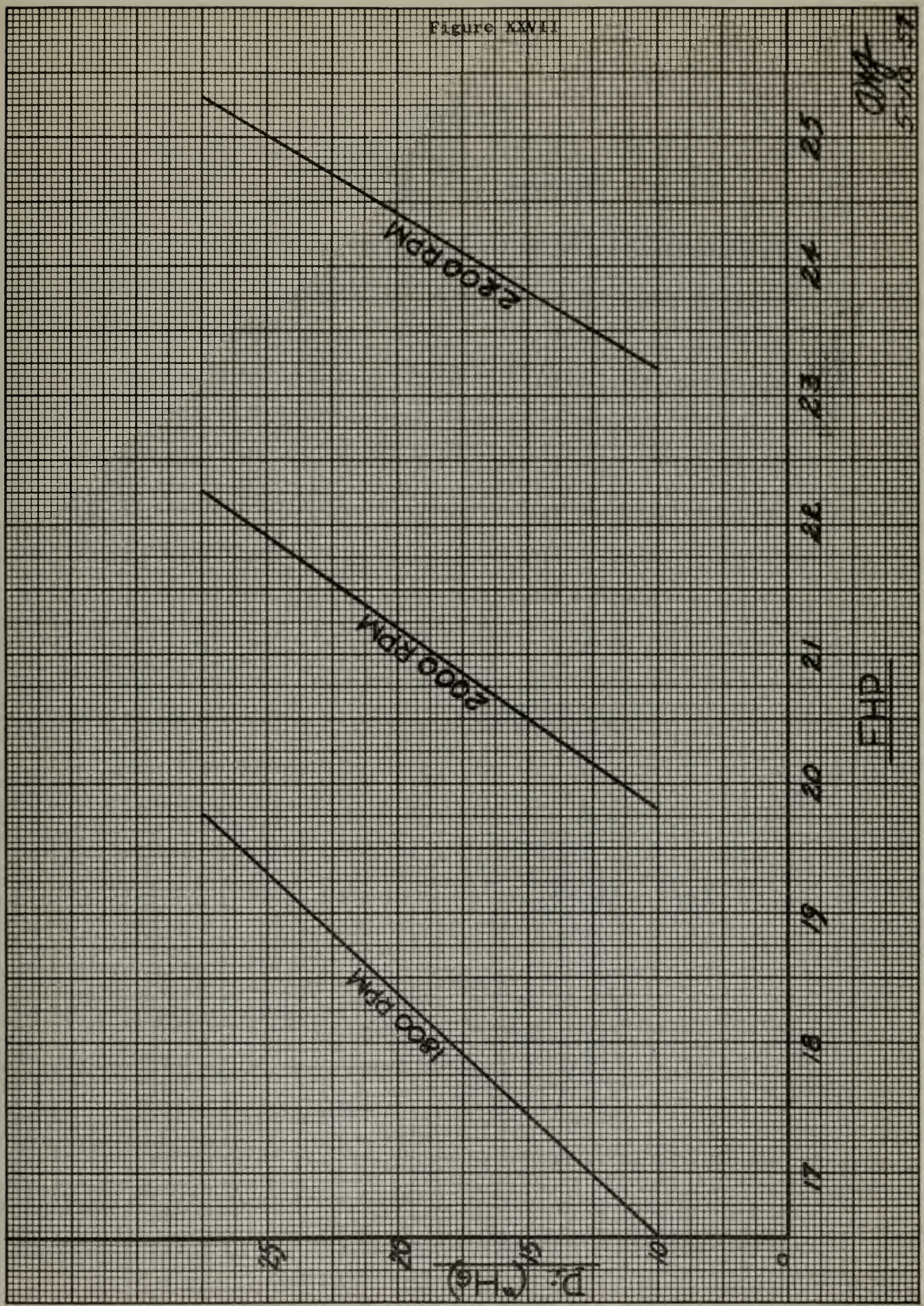

APPENDIX G

SUPPLEMENTARY DISCUSSION

The following is a summary of experimental and instrumentation techniques that is recommended if a similar setup were to be used for further experimentation.

1. Static and stagnation pressure pickups in the exhaust pipe.

Some fouling of the static pressure pickups was encountered when motoring. This can be avoided by placing these pickups on the side of the pipe in a horizontal position instead of vertically on the bottom of the pipe.

A new design of the stagnation probes should be made, so as to have a positive means of alignment to permit changing these stagnation pickups while running. The best place for the stagnation pickups still seems to be in a vertical position on top of the pipe.

2. Exhaust pressure in the pipe.

An extra static tap should be made in the pipe and attached to a manometer. This is a necessity to enable any quick calculation of the scavenging density, since this is based on exhaust pressure from the engine.

3. Engine operating oil temperature.

Some means should be made to measure the oil temperature of the engine. This would permit a more accurate check on the friction losses.

4. Balancing the engine.

Some trouble was encountered in attempting to balance this engine when operating it as a one-cylinder engine. The ideal way to balance would be to remove two pistons with their connecting rods and

rebalance the engine for the one remaining piston. This was attempted. It was discovered that the original balance weights were on the drive gears of the cam shaft. A redesign of the drive gears would be necessary to take out the original counterweights and balance for only one cylinder operation. Time would not allow this to be done.

Therefore, the original pistons and connecting rods were replaced and the exhaust ports and fuel rack to two of the cylinders were blocked off. This proved to be a satisfactory solution to the balance problem but presented the additional problem of the friction power. The engine now had only one cylinder for brake power but had the same friction power requirements as the original three-cylinder engine. This meant that the brake power from one cylinder operation was of the same order of magnitude as the friction power. This leads to an obvious source of error which with care can be kept to a minimum. The best way to eliminate this error is to take cylinder cards at each run and calculate the indicated mean effective pressure from a p-v diagram made from these cards. Knowing the brake mean effective pressure, an accurate measure of the friction mean effective pressure is obtained.

5. Recommended method of operation of the engine.

It became apparent only after the test runs were made and the data and calculations plotted that there is one particular way of operating this engine which provides a most efficient means of recording the exact data necessary. The following is a summary of the recommended method of operation should future experiments be made with this setup. These steps should be followed in more or less consecutive order. Whether the engine must be run as an engine or motored depends, of course, on the fuel-air ratio under consideration. This outline will consider the

normal operating case of running as an engine. For a detailed explanation of the calculations see Appendix D.

a. Start the engine with no load or light load, and allow the engine to come up to temperature at a fast idle speed around 1000-1200 rpm.

b. Bring the engine up to desired speed.

c. Set up the scavenging ratio desired by:

   (1) Measuring the air flow (P_1, Pi, ΔP).

   (2) Measuring the scavenging density (T_1 and P_{E_1}).

   (3) Adjusting until the desired R_S is obtained. Care must now be taken to insure that these conditions remain constant during the run. This is done by adjusting ΔP with a bleeder valve.

d. Set up the fuel-air ratio desired by metering the amount of fuel necessary with the fuel throttle valve while adjusting the brake load to maintain the desired rpm, and adjusting ΔP if necessary to restore the scavenging ratio.

e. Since the fuel-air ratio and scavenging ratio are now set and since the rpm has been adjusted by varying the load, all readings and indicator cards may now be taken.

f. Having completed the data point in question, two more runs should be made with the identical set up, varying the fuel flow a little above and a little below the original point. Adjust the load each time to keep the rpm constant.

g. Having completed these three runs, the data point desired has been spotted and bracketed. This will enable a cross plot to be done accurately and with a minimum of test runs. This completes one data point.

h. Repeat the above steps for every data point desired. It is felt that for every scavenging ratio, three data points covering fuel-air ratios of 0.02, 0.03, and 0.04 are necessary. Since three runs are required for each data point, a total of nine runs completes the full range of fuel-air ratios at any chosen scavenging ratio.

APPENDIX H

BIBLIOGRAPHY

1. Brosens, Pierre J. - Introductory Analysis of the Scavenging Process in Two-Stroke Engines, MIT Masters Thesis, 1956

2. Dean, Miles - Techniques for Protecting and Waterproofing Resistance Wire Strain Gauges, David Taylor Model Basin, Report 797, March 1956

3. Houtsma, C. G., Howarton and Working - Relation of Scavenge Efficiency in the Two-Stroke Compression Ignition Engine, MIT Thesis, 1950

4. Keenan, J. H. and J. Kaye - Gas Tables, Wiley, 1945

5. Leary, Wm. A. and D. H. Tsai - Metering of Gases by Means of A.S.M.E. Square Edged Orifice with Flange Taps

6. Murray, Wm. M. and P. K. Stein - Strain Gauge Techniques, 1956, Part II, Chapter 12

7. Shapiro, A. H. - The Dynamics and Thermodynamics of Compressible Fluid Flow, Vol. I, Ronald Press, 1955

8. Perry, C. C. and H. R. Lissner - The Strain Gauge Primer, McGraw-Hill 1955

9. Taylor, C. F. and A. R. Rogowski - Scavenging of the Two-Stroke Engine, SAE Transactions 1954, pp. 486-498

10. Taylor, C. F. and E. S. Taylor - The Internal Combustion Engine, International Textbook Company, 1938

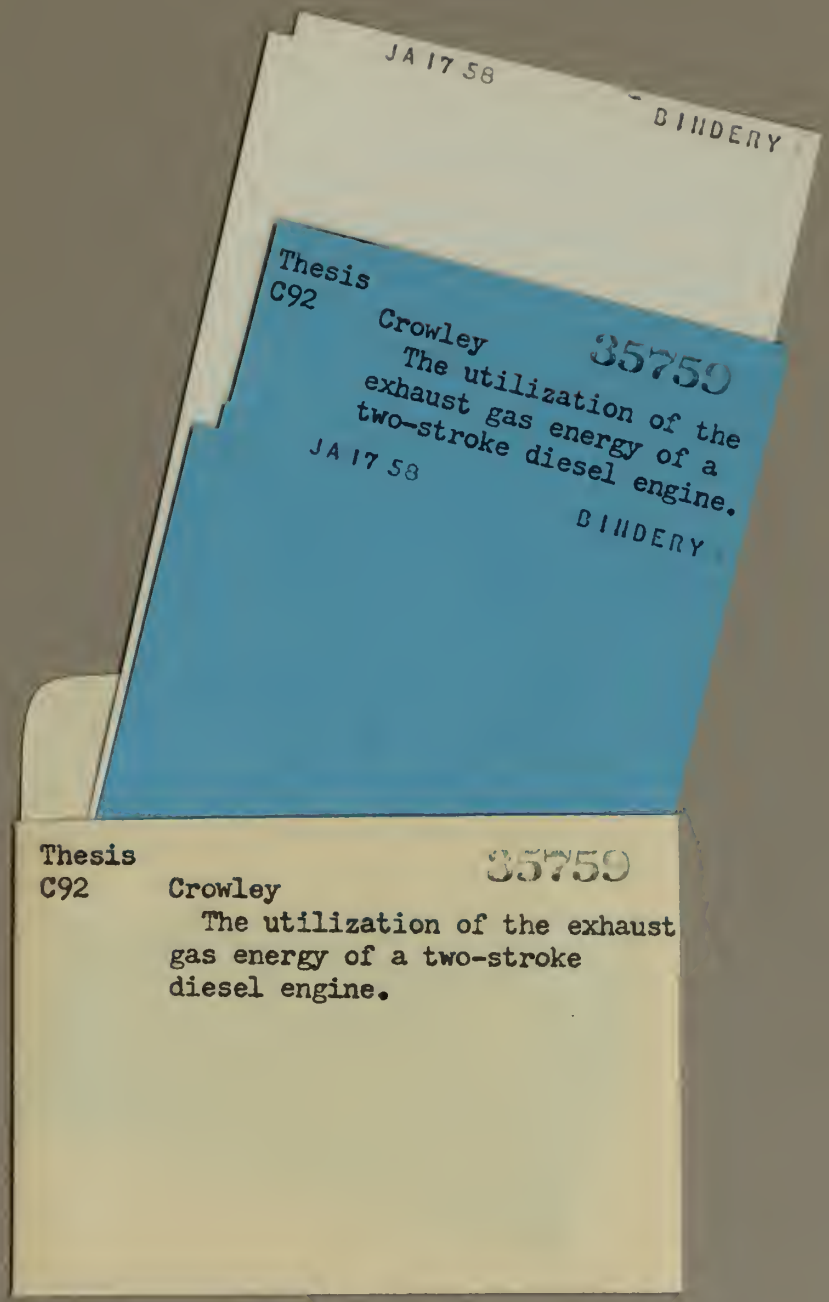
JA 17 58
BINDERY
Thesis
C92
Crowley
35759
The utilization of the exhaust gas energy of a two-stroke diesel engine.
JA 17 58
BINDERY
Thesis
C92
Crowley
35759
The utilization of the exhaust gas energy of a two-stroke diesel engine.

thesC92
The utilization of the exhaust gas energ
3 2768 002 08958 3
DUDLEY KNOX LIBRARY